Exploring advances in nanofiber-based face masks: a comprehensive review of mechanical, electrostatic, and antimicrobial functionality filtration for the removal of airborne particulate matter and pathogens

Emergent Materials (2024) 7:765–800
https://doi.org/10.1007/s42247-023-00622-9

REVIEW

Exploring advances in nanofiber-based face masks: a comprehensive review of mechanical, electrostatic, and antimicrobial functionality filtration for the removal of airborne particulate matter and pathogens

Bao Le[1,2] · Nada Omran[3] · Eman Elnabawy[1] · Ahmed H. Hassanin[3,4,5] · Kamal Mahmoud[3,6] · Nader Shehata[3,6,7,8,9] · Islam Shyha[1]

Received: 13 August 2023 / Accepted: 24 December 2023 / Published online: 16 January 2024

Abstract

The filtration of airborne particulate matter (PM) and aerosols utilizing nonwoven fibrous materials has received significant research concern due to the continuing global pandemics, especially the outbreak of coronavirus disease (COVID-19), and particularly for face masks as a measure of personal protection. Although spun-bond or melt-blown nonwoven fabrics are among the pioneer materials in the development of polymer microfiber-based face masks or air filters on a large scale, relatively new nonwoven manufacturing processes like electrospinning and solution blow spinning (SBS) are gaining momentum among manufacturers of filter membranes. The high filtration performance of nanofiber face masks is due to their high surface area to volume ratio which increases the interaction between the nanofiber and PM and improves the electrostatic charge distribution of electret filters, allowing enhanced capture capability based on electrostatic deposition. Moreover, the small diameter of nanofibrous filters improves the breathability of the face mask by providing the slip effect, which in turn reduces the pressure drop through the membrane. This paper provides a comprehensive review of contemporary advances in nanofiber face masks, detailing the working mechanism involved, reviewing recent experimental studies, and discussing improvements in filtration efficiency for three main nanofibrous air filtration strategies, including mechanical and electrostatic filtration and antimicrobial functionality. Furthermore, prospective research is introduced which considers the synergistic combination effects of the three filtration mechanisms in designing a multifunctional nanofiber structure that can efficiently capture a wide range of PM with higher filtration efficiency and lower drops in pressure. New trends in the antimicrobial activity of smart material-based nanofibrous membranes in the fight against infectious airborne agents are also described.

1 Introduction

Anthropogenic air pollution has a considerable negative impact on public health. Particulate matter (PM) contains microscale airborne contaminants and is acknowledged to be a significant risk factor for early death [1]. The most well-known sources of the negative health consequences of PM are toxicological effects brought about by direct inhalation. Toxic chemicals contained in PM which are often hazardous to cells and capable of causing cell death or organ failure

✉ Eman Elnabawy
e.elessawy@napier.ac.uk

1 School of Engineering and the Built Environment, Edinburgh Napier University, Edinburgh, UK

2 Faculty of Engineering, Vietnamese-German University, Ben Cat, Binh Duong, Vietnam

3 Center of Smart Materials Nanotechnology and Photonics (CSMNP), Smart CI Research Center, Alexandria University, Alexandria 21544, Egypt

4 Department of Textile Engineering, Faculty of Engineering, Alexandria University, Alexandria 21544, Egypt

5 Wilson College of Textiles, North Carolina State University, Raleigh, NC, USA

6 Department of Engineering Mathematics and Physics, Faculty of Engineering, Alexandria University, Alexandria 21544, Egypt

7 Kuwait College of Science and Technology (KCST), 13133 Doha District, Kuwait

8 Faculty of Science, USTAR BioInnovations Center, Utah State University, Logan, UT 84341, USA

9 School of Engineering, Ulster University, York Street, Belfast, Northern Ireland BT15 1ED, UK

are metals, nitrates, and sulfates. Moreover, PM2.5 particles, which have aerodynamic dimensions less than 2.5 mm, can freely enter the circulatory system and increase the risk to health [2]. These harmful health effects of PM have increased awareness of the toxicological impacts of inhaling PM. Also, small particles that have high surface-to-volume ratios may adsorb aerosols containing viruses and have high surface-to-volume ratios, thereby further contributing to the spread of different viral infections [3]. The coronavirus disease (COVID-19) pandemic has recently focused attention on these PM-related concerns, and SARS-CoV-2 (severe acute respiratory syndrome coronavirus-2) viral RNA has been found on the surface of aerosols (≤ 5 µm) collected from public areas (Fig. 1) [4]. Moreover, according to ecological research, even a small increase in chronic PM2.5 exposure might cause a significant rise in COVID-19 mortality [5].

Therefore, the control of air quality has become a vital component in maintaining sustainable public health. The most popular approach for air purification among many available options is PM filtration, which uses filtering material to remove airborne particles. Membranes and fibrous materials are among the common candidates for use as air filters [7, 8]. These air filters are evaluated based on a variety of performance criteria, and one crucial measure that represents how effectively particles are removed is filtration efficiency. Another crucial indicator of how easily the airflow can pass the filtering media is the pressure drop which indicates the breathability of face masks. However, a trade-off between these two criteria is a main issue in research on air filters and has led to research interest in developing nanofiber air filters to promote airflow while effectively capturing particulates based on either mechanical filtration, electrostatic charge, or antimicrobial functional air filters (Fig. 2).

In the mechanical filtration process, aerosol particle filtration depends on several factors, including nanofiber diameter, airflow velocity, and PM particle size [9]. Particulate pollutants with varying particle sizes are filtered from the air stream by interception, Brownian diffusion, and inertial impaction [10]. These methods rely mainly on the design and structure of the air filter to physically capture PM by disrupting the smooth laminar airflow or streamlines passing through the material [11]. In the case of particles larger than 0.3 µm, both inertial and direct impact exert significant influence, while for particles of 0.1 µm, diffusion stands as the primary filtering mechanism. The particle size at which the separation membrane achieves its lowest efficiency is commonly referred to as the "most penetrating particle size," which typically falls within the range of 0.3 µm or smaller [12].

Several studies have reported the efficiency of nanofiber membranes in improving the filtration performance of face masks by controlling their pore size [13–15]. The effective interconnection of the pores leads to enhancements in diffusion, inertial effects, and interception as well. However, conventional nanofiber air filters still face certain challenges due to their small pore size and significant thickness, which result in high filtration efficiency but also lead to substantial pressure drops. This, in turn, leads to an overall reduction in

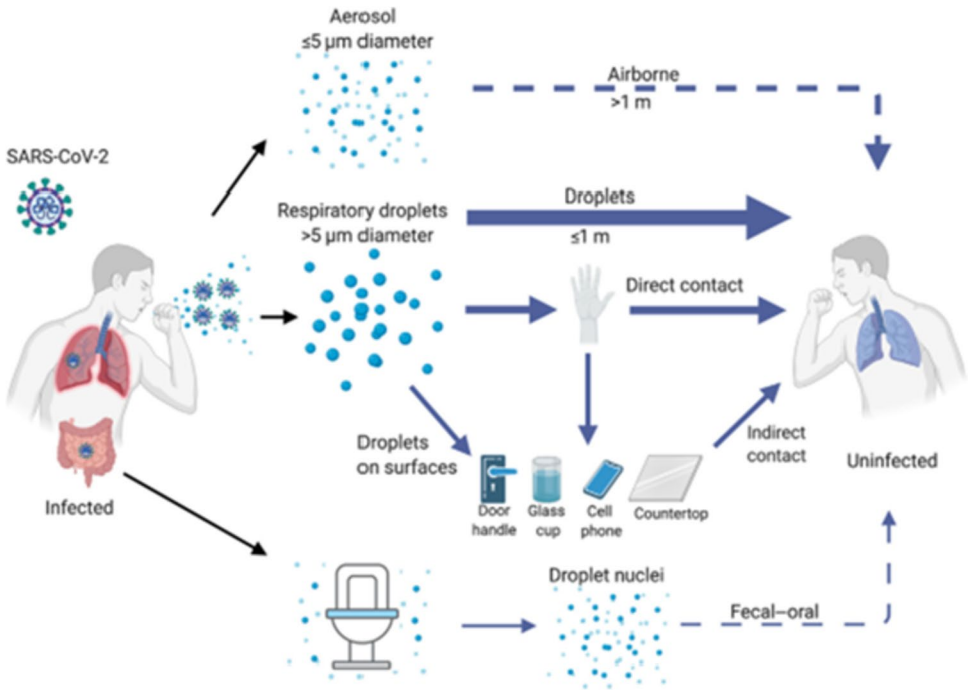

Fig. 1 Proposed severe acute respiratory syndrome coronavirus-2 (SARS-CoV-2) transmission routes [6]

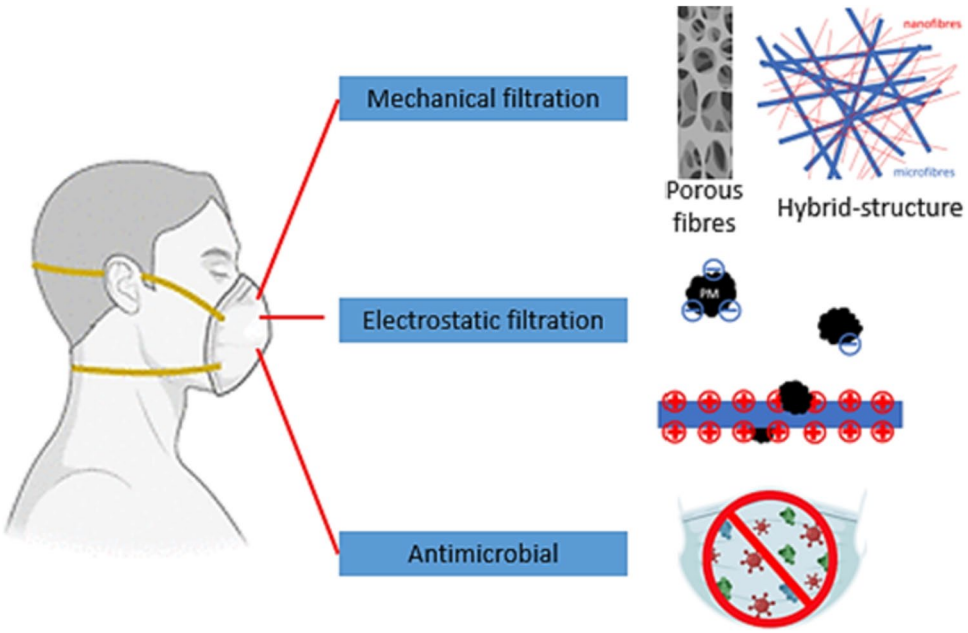

Fig. 2 The advancement in nanomaterials for face masks

filtration performance [16]. In contrast, electrostatic attraction primarily relies on electrostatic interactions between particles and the filtration media, without significantly affecting airflow [17–19]. Consequently, by optimizing the filter structure and enhancing the electrostatic interactions, it becomes possible to achieve a balance between filtration efficiency and pressure reduction, ultimately leading to improved filtration performance.

Electrostatic filtration has been widely reported in the literature achieved using different mechanisms including induction charging [20], triboelectric charging [21], or corona charging [22, 23]. Electret nanofiber membranes refer to materials that are electrically activated and can generate a quasi-permanent electric field on their own. Electret filters are created by introducing electric charges into the material or aligning electric dipoles within the dielectric material [24]. Numerous research studies have focused on the enhancement of air filter performance by elevating surface potential and extending the lifespan of their electrical properties in order to improve the durability and lifetime of nanofiber face masks [25].

Additional crucial hazards for human health are pathogenic organisms [26] in the form of viruses, fungi, or bacteria [27]. These organisms represent the major factor causing infectious diseases in humans and other animals. Recent statistics indicate that approximately one-quarter of annual global deaths can be attributed to these pathogenic agents [28]. According to the World Health Organization (WHO), respiratory illnesses arising from annual seasonal influenza lead to around 290,000 to 650,000 deaths each year [29]. Therefore, the need for antimicrobial face masks has become an urgent requirement for human health and represents an appealing alternative to conventional face masks which could help address some of the concerns associated with single-use face masks by providing real-time, in situ antimicrobial protection [30, 31]. The feasibility of the use of nanofiber for functionalization and chemical modification, as well as the ability to incorporate natural antimicrobial polymers in the spinning process, makes it a perfect candidate for the fabrication of usable, flexible, and highly efficient antimicrobial face masks [32, 33].

In this review, the advances made in nanofibrous face masks are summarized based on three distinct categories of mechanical filtration, electrostatic filtration, and antimicrobial functionality (Fig. 2). All new research approaches that aim to enhance the filtration performance of nanofibrous membranes based on these three filtration classifications are discussed in detail. The future prospects of the hybridized filtration effects in improving the durability, cyclability, and lifetime performance of nanofibrous face masks are then considered. Combating airborne pathogens using functionalized antimicrobial nanofiber either through the use of doping, coating, or mixed matrix composites to proactively deactivate pathogens is also discussed.

2 Mechanical filtration

2.1 Experimental work related to mechanical filtration

Applications of nanofibrous membranes have been experimentally proven to improve particle filtration performance compared to nonwoven microfibers [34]. Nanofiber

membranes provide high surface area due to their high aspect ratio (length/diameter) and small pore sizes that contribute to increasing particle-capture ability and high filtration efficiency [35]. Also, their low basis weight or packing density can lower pressure drops and air resistance [36]. In general, the filtration performance of a filter media in terms of mechanical filtration depends on various factors that can be categorized into two main groups: (I) filter structure, including membrane pore size and porosity, and (II) filtration conditions including humidity, temperature, PM source, and face velocity. To improve the filtration performance of nanofibrous mats, research in this field has mostly focused on filter structure, with various attempts to attain smaller pore sizes by reducing nanofiber diameter or increasing filter thickness while still maintaining high porosity to reduce the drop in pressure. This section discusses recent experimental studies related to mechanical air filtration and the modification of nanofiber structures in order to attain higher filtration efficiency [37].

One of the most convenient methods in mechanical filtration to improve air filtration performance is to control membrane pore size by altering the nanofiber diameter. Reducing the diameter has been experimentally proven to improve filtration efficiency and reduce pressure drops. An early experimental study by Skaria et al. found a substantial decrease in airflow resistance of 82%, accompanied by a comparable filtration efficiency of 84% for nanofiber filters in contrast to commercial N95 respirators [38]. Most nanofiber air filters are produced by the electrospinning technique, where fiber diameter and pore size can be controlled by changing the concentrations of polymer used or adjusting process parameters such as voltage, working distance, and flow rate. A recent study by Bian et al. of the effect of nylon solution concentration in controlling the diameter of the nanofiber generated indicated that the filtration efficiency of PM2.5 was significantly enhanced with decreasing nanofiber diameter regardless of the face velocity applied (Fig. 3a) [39]. A denser nanofiber filter network with a small pore size of < 70 nm showed a higher PM removal efficiency of up to 96%. However, the dependence of removal efficiency became less sensitive at high spinning times of 3 or 4 h due to the dominance of layer thickness in capturing particles.

Similarly, an experimental study of the filtration performance of polyethylene terephthalate (PET) nanofibrous

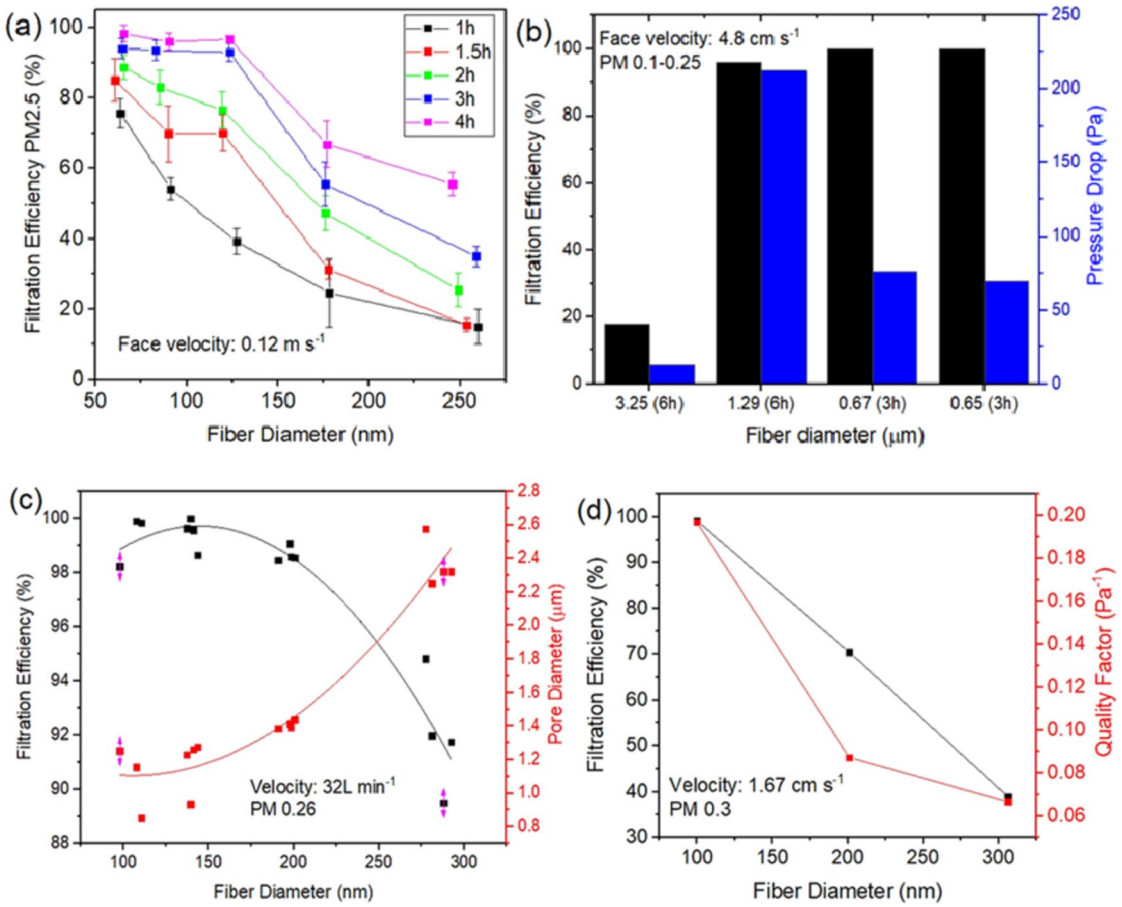

Fig. 3 Relationship between PM2.5 removal efficiency and nanofiber diameter **a** [39], **b** [40], **c** [41], and **d** [42]

filters demonstrated a significant increase in filtration efficiency from 41 to 99% when the nanofiber diameter was reduced from 3.25 to 0.67 µm (Fig. 3b) [40]. The reduction in nanofiber size was achieved by decreasing the PET concentration from 20 to 10 wt% and using a smaller needle size of 0.3 mm rather than 0.7 mm. Filter membranes comprising finer nanofiber exhibited a notable 97% reduction in pore size compared to larger diameters, which subsequently contributed to enhanced mechanical filtration efficiency. Consequently, this study proposed various approaches involving the manipulation of nanofiber diameter, morphology, and filter thickness so as to achieve more efficient filter media with low pressure reductions. These adjustments could be implemented through modifications of polymer concentration, needle size, and electrospinning parameters, including the rotation speed of the collector and processing time. The effect of reducing polymer concentration on attaining finer nanofiber, smaller pore size, and consequently better filtration efficiency was also experimentally addressed by Wei et al. (Fig. 3c) [41]. This study also highlighted the significant role of narrower nanofiber diameter and pore size distribution in enhancing the mechanical filtration performance of nanofibrous filter media resulting from reducing the polymer concentration. However, due to the decreased membrane pore size, the pressure drop negatively increased which caused greater air resistance and a lower quality factor. The effect of nanofiber diameter on the relationship between filtration efficiency and pressure drop is still not justified. The reduction in nanofiber diameter should theoretically enhance the mechanical filtration efficiency since the filtration coefficients of inertial impaction, interception, and diffusion mechanisms increases with decreasing pore size. Meanwhile, following the slip effect, we could conclude that a smaller nanofiber diameter would also reduce the pressure drop. However, based on Davies's equation (Eq. 5), decreasing the nanofiber diameter results in a higher pressure drop. Based on both theoretical and experimental adaptions, Kim et al. [42] have claimed that, although the pressure drop increased, the quality factor was still enhanced at smaller nanofiber diameter due to a noticeable increase in filtration efficiency (Fig. 3d). Based on all of the relevant studies mentioned, it can generally be concluded that the use of finer nanofiber contributes to the high filtration efficiency of filter media, but the reduction in pressure drop has still been controversial. Therefore, the employment of a bilayer system containing a micro-fibrous polypropylene (PP) substrate and a nanofibrous facial layer has been shown to contribute to a considerable enhancement in filtration efficiency compared to micro-fibrous bilayers, especially in the range of most penetrating particle size (MPPS) of 10–500 nm with only a moderate rise in pressure drop [43]. This led to a significant increase in quality factor up to 2.6 times higher than that of its micro-fiber counterpart. Similarly, a comparative study of a gauze mask incorporating nanofiber and other commercial micro-fiber face masks has indicated an effective filtration of nanofibrous filter for PM2.5 particles (90%) while preserving a relatively low pressure drop (0.41 kPa) compared to the ITO PM2.5 micro-fiber mask (82.8%/0.655 kPa) [44]. The high porosity of nanofiber with its small micro-pores is the main reason for the enhanced mechanical filtration performance [38]. Moreover, a multi-structured bio-based polylactic acid (PLA) nanofibrous membrane could maintain its natural biodegradability and high filtration efficiency > 99.99% for PM0.3 when exposed to a humid environment of 90% humidity up to 100 h [45].

However, although nanofibrous filters can provide high removal efficiency, an accompanying breathing obstruction in face masks is unavoidable. Breathability is mainly related to the pressure drop, which is a function of the basis weight of the membrane filter. Therefore, it is important to identify the optimal basis weight of the membrane in which both high filtration efficiency and low pressure drop or an optimal quality factor can be achieved [46]. One experimental study has found that an optimal quality factor of around 0.061 Pa^{-1} for a TPU nanofiber membrane could be obtained at a basis weight of 6 $g.m^{-2}$ [47]. This nanofiber net can achieve a removal efficiency of around 97% for both PM0.1 and PM2.5 with a low pressure drop of ~ 58 Pa at an airflow rate of 1.0 $L{\cdot}min^{1}$. Another experimental investigation indicated that the increasing packing density of the nanofibrous filter significantly reduced the MPPS from 140 to 90 nm, while the filter thickness had an unobvious effect on the filtration performance of polyethylene oxide (PEO) nanofiber with an average diameter of 208 nm [48] (Fig. 4).

Another multi-level polyacrylonitrile/graphene oxide (PAN/GO) nanofibrous membrane has been developed to remove ultrafine particles (100–600 nm), and the composite membrane exhibited excellent improvement in filtration performance for PM0.3 compared to the neat PAN nanofibrous membrane [50]. Its high porosity, small pore size, and optimal surface chemistry contributed to the outstanding performance of this nest-like multi-level structured membrane (Fig. 5a). It was also claimed that the use of nanofiber led to the reduction of the drop in pressure due to the slip effect. Similarly, another modified structure in a PA6 nanofibrous membrane has also shown a significant enhancement in filtration performance [51]. It contains a 2D PA6 nanonet layer with Steiner tree structures embedded in a nonwoven PET scaffold substrate (Fig. 5b), resulting in a ripple-like membrane. The addition of PET filament helps to extend the frontal surface of the PA6 nanofibrous membrane by lengthening its pleat span and pitch. This gives it a highly porous structure with extremely small pore size (0.6–0.7 µm) and low basic weight (0.9 g m^{-2}), consequently contributing to low air resistance (37 Pa), high filtration efficiency (~ 99%), and a robust quality factor (> 99%). A further advance is that

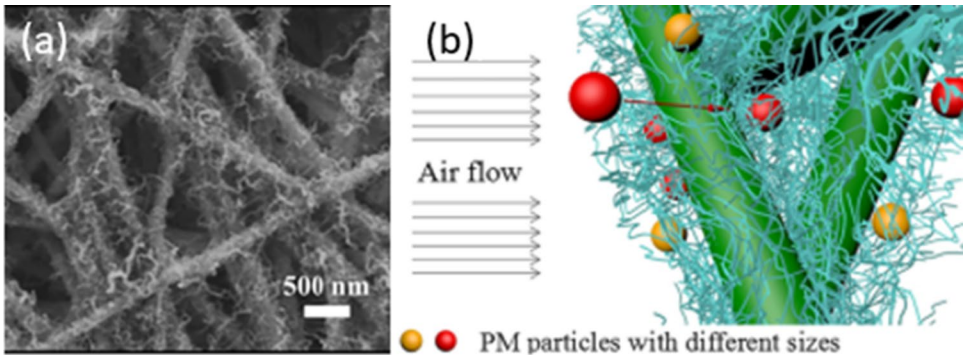

Fig. 4 Hybrid structured nanofiber-based filters: **a** SEM images of PMIA/SiO2-NFs nanofiber and **b** its schematic illustration of the PM2.5 removal process (Reproduced with permission from [49], Copyright Elsevier 2018)

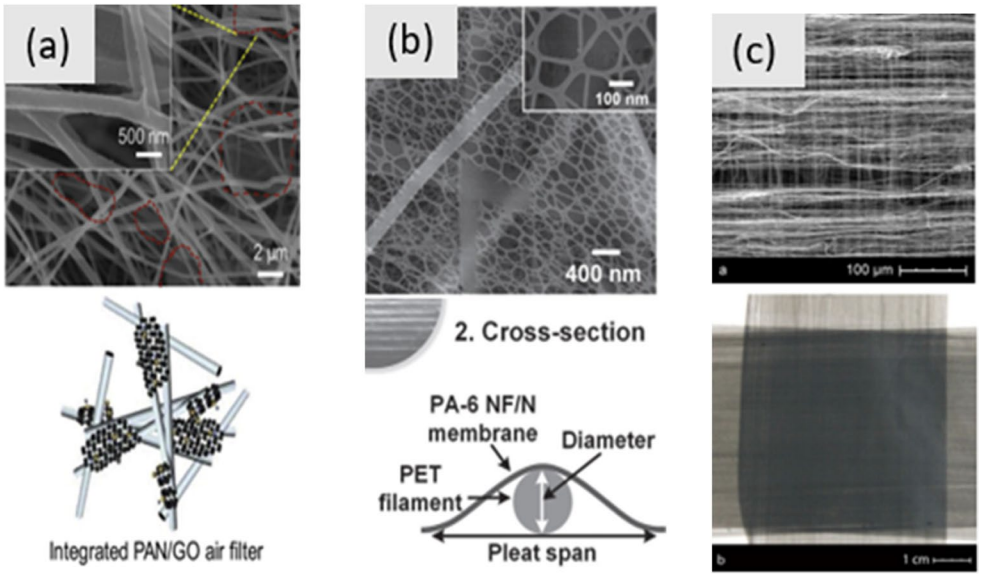

Fig. 5 Various types of hybrid structured nanofiber-based filters: **a** integrated PAN/GO filter [50], **b** a ripple-like membrane of PA-6 NF/PET [51], and **c** a cross-plied structured membrane with CNTs (Reproduced with permission from [54], Copyright Elsevier, 2013)

this structure employs a polyacrylonitrile (PAN) nanofibrous scaffold substrate instead of conventional nonwoven fabric [52, 53]. 2D ultrafine PAN nanonets (20–30 nm) fabricated by electrospinning/netting are bonded with the scaffold, and the resulting membrane exhibited extremely high filtration efficiency up to > 99.99% for PM0.3 due to the diameter of the ultrafine nanofiber and small pore size (< 300 nm). Also, its high porosity (~ 93%), low filter thickness (~ 0.4 μm), ultra-light base weight (0.68 g m^{-2}), and low packing density result in a low pressure drop of 73.5 Pa. Another adaptation is the use of a cross-plied structured membrane with carbon nanotubes (CNTs) [54]. Three cross-plied CNTs layers integrated into nonwoven PP fabric (Fig. 5c) provide higher filtration performance with a low particle penetration of 0.1% for PM0.3 and a comparable pressure drop of 200 Pa. The extremely small diameter and low packing density of CNTs were hypothesized to contribute to the superior filtration performance of this kind of nanofibrous membrane compared to conventional nanofiber filters. However, any further increase in the number of CNTs layers (up to 7 layers) led to the filter exhibiting higher air resistance.

2.2 Mechanisms of mechanical filtration

The physical or mechanical filtration mechanisms comprise inertial impaction, interception, and diffusion. The filtration mechanism is mostly a function of particle and nanofiber size and flow velocity [55]. As shown in Fig. 6a, the filtration efficiencies of both the impaction and interception mechanisms exhibit their highest values (> 99%) for medium-sized particles (1–10 μm), but these levels are dramatically reduced for particle sizes below that range. In contrast, variations in filtration efficiency in the diffusion filtration regime lead to the opposite trend, with excellent filtration performance for ultrafine particles (< 1 μm) but lower efficiency as particle size increases. This results in a typical U-shaped curve which indicates the least efficient filtration at a specific range of particle size (the bottom of the U-shaped curve) which represents the most penetrating particle size (MPPS) [56]. This value can be observed from Fig. 6a to be a particle size of 0.3 μm. The MPPS measure is commonly referenced in standard filtration tests due to its highest possibility to penetrate the filter media

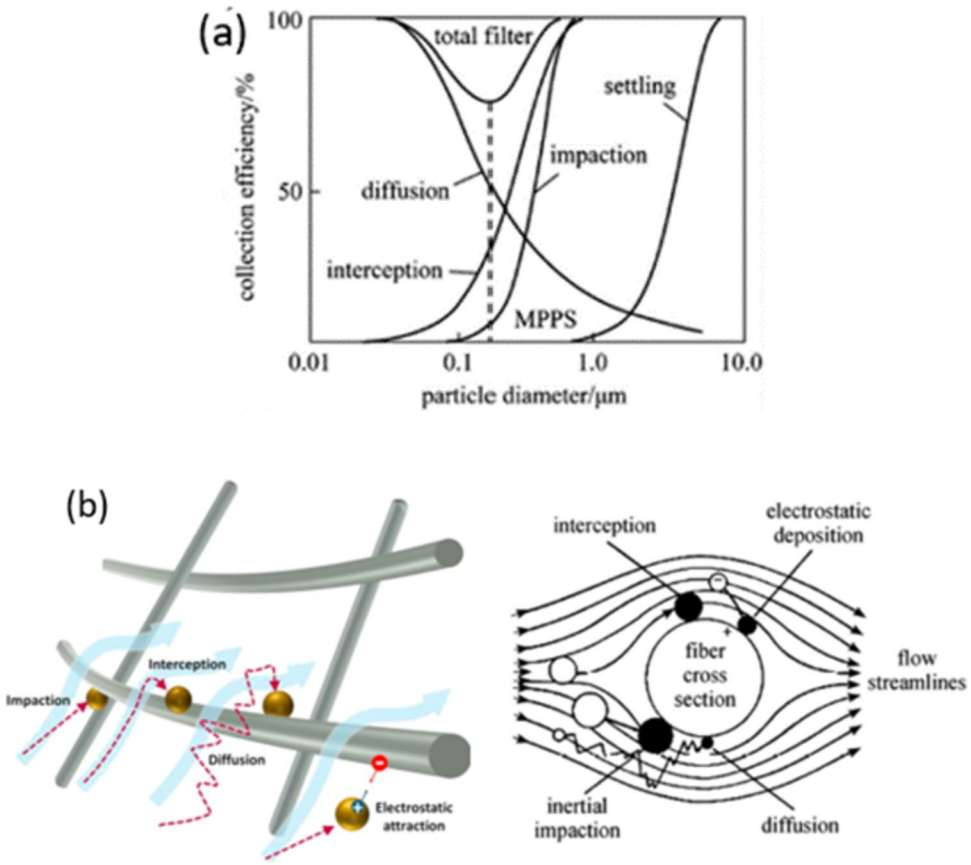

Fig. 6 **a** Collection efficiency of various air filtration mechanisms as a function of particle size (Reproduced with permission from [57],Copyright Elsevier 2012). **b** Mechanisms of particulate matter filtration by nanofiber (Reproduced with permission from [11], Copyright Elsevier 2021)

compared to other particle sizes. These different variations of filtration efficiency in mechanical filtration mechanisms are explained in the following subsections.

2.2.1 Inertial impaction

Inertial impaction is the predominant filtration mechanism for large particles > 1 μm in diameter [58, 59]. This mechanism occurs when a particle is not able to follow the streamline direction near a nanofiber due to its inertia. The particle, therefore, continues to move along its original path and contacts the elements of a filter (Fig. 3b). Inertial impaction depends on the flow velocity (u) and nanofiber size (d_f) and can be expressed by the dimensionless Stokes number [60]:

$$St = \tau \frac{u}{d_f} \tag{1}$$

where τ is the relaxation time of a particle (s), u is the flow velocity (m.s^{-1}), and d_f is the diameter of the nanofiber (m). Inertial impaction is predominant when (St > 0.5). In other words, this mechanism is significant for large (or heavy) particles and/or small nanofibers at high flow velocities which generate high inertia in particles [61].

2.2.2 Interception

Interception occurs when particle size is further reduced to submicron level (0.1 to 1 μm) [62, 63] and can reach 0.6 μm [64]. When such small particles move along the streamline, they are captured by the nanofiber when the streamline approaches to a distance within one particle radius (Fig. 3b). In other words, the particles that move along the streamline close to the nanofiber at or below that distance are hindered by Van der Waal's force [65]. Larger particles cannot contact the nanofiber owing to hydrodynamic repulsion. The single nanofiber interception collision coefficient (E_R) can generally be expressed as

$$E_R = \frac{d_p + d_f}{d_f} \approx \frac{d_p}{d_f} \left(d_p \gg d_f\right) \tag{2}$$

where d_p is the particle diameter and d_f is the nanofiber diameter (both in m).

2.2.3 Diffusion

Further reductions in particle size to below 0.3 μm result in the dominance of diffusion. Based on the kinetic theory of

gases, air molecules tend to collide with each other, causing random motions on zigzagging paths between them, namely, Brownian motion [66]. Due to their interaction with air molecules, such small particles also exhibit Brownian motion, leading to a randomly suspended state. The zigzagging motions of the small particles near the nanofiber lead to their diffusion down a concentration gradient and, consequently, they adhere to the nanofiber surface (Fig. 3b). The diffusion coefficient can be identified based on the Stoke-Einstein equation [67]:

$$D = \frac{kT}{6\pi\eta r_p} \tag{3}$$

where D is the diffusion coefficient (m^2s^{-1}); k is the diffusion coefficient for a particle in a free volume which is a function of the Boltzmann constant, J K^{-1}; T is the absolute temperature (K), η is the viscosity of the solution ($kg{\cdot}m^{-1}{\cdot}s^{-1}$); and r_p is the hydrodynamic radius of the particle (m). The diffusion mechanism becomes noticeable as the particle size is reduced, especially at low face velocity [68]. Lower speeds lead to a longer residence period of the particles, increasing the probability of particle-fiber collisions [69].

2.3 Theoretical work related to mechanical filtration

The advantages of the use of nanofibrous filter media compared to micro-counterparts in improving filtration efficiency can be explained theoretically based on the nature of the processes involved in mechanical filtration [43]. The theory of aerosol particles through a single fibrous filter indicates that a decrease in nanofiber diameter (d_f) will lead to an increase in the Stokes number (St) as well as the single-fiber interception collision efficiency (E_R), as shown in Eqs. 1 and 2, respectively. As a result, improvements are seen in inertial impaction and interception filtration efficiency. Furthermore, the coefficient of diffusion of particles is independent of nanofiber diameter, as shown in Eq. 3, but the particle size. However, a reduction in nanofiber diameter results in the decrease of the Peclet number (P_e), which is the ratio between convection and diffusion transport as shown in the following equation [70]:

$$Pe = \frac{\text{Convection}}{\text{Diffusion}} = \frac{u.d_f}{D} \tag{4}$$

where P_e is dimensionless and u is the face flow velocity ($m.s^{-1}$), d_f is the nanofiber diameter (m), and D is the diffusion coefficient ($m^2.s^{-1}$).

It can be seen from Eq. 4 that a smaller nanofiber diameter (d_f) leads to a reduction in P_e, and consequently the domination of the diffusion mechanism. Therefore, the use of nanofiber can be theoretically proven to enhance mechanical filtration efficiency [61]. A theoretical approach to the investigation of the filtration performance of electret fibrous filters in particulate respirators has indicated a significant increase in both filtration efficiency and the quality factor due to the reduction in nanofiber diameter (Fig. 7) [71]. At nanoscale, it has been claimed that electrostatic capture is improved due to the reduction in

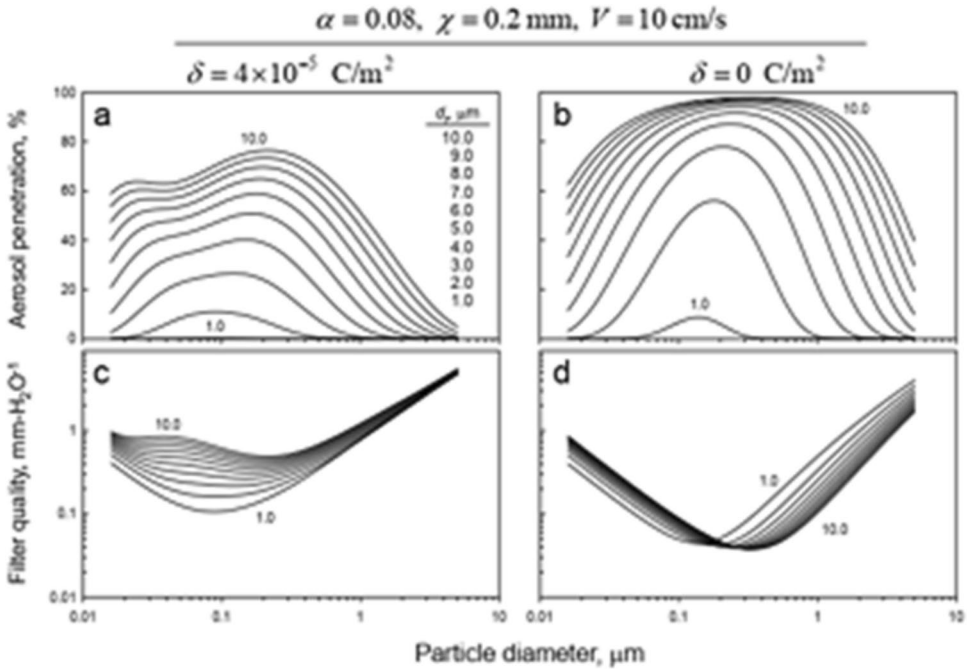

Fig. 7 Effect of nanofiber diameter on aerosol penetration and filter quality [71] (Open access)

nanofiber diameter from 525 to 82 nm when filtering airborne coronavirus in masks and respirators [62].

Furthermore, the benefits of reducing the diameter of nanofiber in filter media can also be expressed in terms of the pressure drop. It is well known that reducing the nanofiber diameter leads to an increase in the pressure drop, and the relationship between nanofiber size and pressure drop can be expressed by Davies's equation [67]:

$$\Delta P = \frac{64\mu u\alpha^{\frac{3}{2}}L}{d_f^2\left(1+56\alpha^3\right)} \tag{5}$$

where ΔP is the pressure drop (Pa), μ is the viscosity (Pa. s), u is the flow velocity (m.s^{-1}), α is the nanofiber packing density in the filter, and L represents the membrane thickness (m). However, smaller sizes of nanofiber in the submicron range lead to better efficiency at the same pressure drop compared to micron level and larger counterparts when continuum (or non-slip) flow is applied [72]. This phenomenon reflects the more dominant effect of reductions in nanofiber diameter compared to pressure drop in increasing filtration efficiency and consequently achieving a better quality factor [71].

Filtration theory assumes that there is no slip condition arises at the nanofiber surface and that a continuous flow is applied in the case of microscale or larger nanofibers. However, this assumption no longer applies when the nanofiber diameter is reduced to the nano-range and the effect of slip flow needs to be taken into consideration [73]. This phenomenon can be explained in terms of the Knudsen layer. This kinetic layer is formed as airflows over a solid face which is a single fiber. When the nanofiber diameter is much larger than the thickness of the Knudsen layer, the effect of the latter is negligible, but it becomes significant when the nanofiber approaches the same order of magnitude of the mean free path of gas (λ). In other words, gas slippage needs to be taken into account in this case, and, subsequently, the non-zero slip velocity (u_s) on the nanofiber surface becomes important (Fig. 8). This slip velocity reduces the drag force when the airflow passes over the nanofiber surface, hence leading to a lower drop in pressure compared to that over micro-fiber. In addition, the non-equilibrium Knudsen layer encompasses a large portion of the total nanoscale pore spaces in this slip flow regime. This means that more of the particles pass close to the nanofiber, hence leading to more particles becoming trapped on the nanofiber surface and better filtration efficiency, especially for diffusion and interception mechanisms involving submicron particles. Therefore, based on the air filtration theory, improvements in terms of filtration efficiency and pressure drop or quality factor can be attained with an increase in the Knudsen number [74–76]. The Knudsen number ($K_n = 2\lambda/d_f$) is employed in order to identify the boundary between different types of flow. A continuum flow appears at $K_n < 0.001$ but is transformed into a slip flow as K_n increases over the threshold of $0.001 < K_n < 0.1$. The nanofiber diameter can be calculated based on these K_n numbers with the specific value of the mean free path of air molecules at room temperature (23 °C) and atmospheric pressure (1.013×10^5 Pa) at around 66 nm [77]. The characteristics of the flow around the nanofiber boundary can be identified using Kuwabara's model [78] taking into consideration the slip effect.

2.4 Efficiency of mechanical filtration

The deterioration in filtration performance in terms of filtration efficiency and pressure drop in mechanical filtration is highly correlated with the flow velocity through the nanofibrous filter network [39]. Experimental research has indicated a reduction in the efficiency of polyamide 6 (PA-6) nanofiber membranes in the filtration of NaCl aerosol particles (PM2.5) at a standard airflow speed of 85 L/

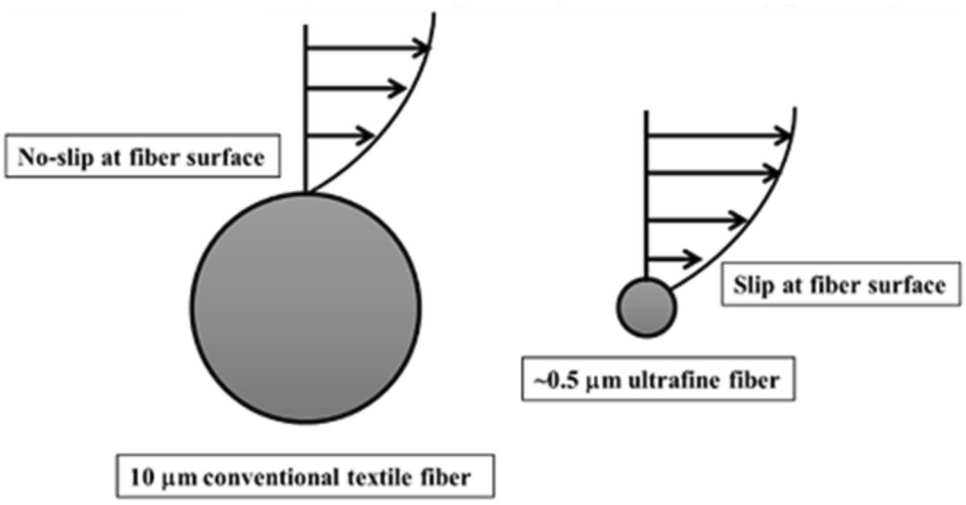

Fig. 8 Slip effect in air filtration using nanofiber in reducing drag force [79] (Open access)

min when the air velocity increases from 0.5 to 0.8 m/min [80]. Increasing flow velocity shortens the residence time of small particles within the filter structure, hence reducing the numbers of particle-fiber collisions and, consequently, diffusion efficiency [48]. However, this reduction in filtration efficiency was much lower for smaller nanofibers below 33 nm in diameter, which showed only a slight decline in efficiency from 99.62 to 86.05% compared to large nanofiber diameters of 120 nm that showed noticeably lower efficiency falling from 99.91 to 60.12%. Small pore size and high surface area are also significant factors in the mechanical filtration efficiency of nanofiber due to their influence in improving interception and diffusion mechanisms [39]. Another crucial factor in mechanical filtration which is closely related to nanofiber diameter is the slip effect, since the slip flow regime in mechanical filtration leads to a significant reduction in the drag force of the air stream, and consequently lower values of pressure drop [76, 81].

Another effective means to lower the pressure drop is to modify the morphology of nanofibers by manipulating conditions in the production process such as flow rate, processing time, and solution concentration. One common approach is to change the morphology of the nanofiber to a "bead-on-string" structure [82–84]. One early study fabricated PLA nanofibrous membranes using this approach [82]. By regulating solvent composition and PLA concentration, the morphology in terms of diameter and bead size of the bead-on-string nanofiber can be controlled (Fig. 9a). The experimental results from this study showed the high filtration efficiency (> 99.9%) of this nanofibrous filter for 260 nm sodium chloride (NaCl) aerosol particles, partly due to the small nanofiber diameter (~ 260 nm) and nanopores on the beads. Also, the presence of beads in this structure increases the porosity of the membrane, leading to the reduction of the pressure drop (165.3 Pa). However, the filtration performance of this kind of membrane deteriorates as face velocity increases, which can be explained by the effects of pore size, packing density, filler thickness, and nanofiber diameter. Therefore, a low face velocity (5.8 cm/s) was recommended so as to attain good filtration performance. The good filtration performance of bead-on-string nanofibrous membranes at low velocities has been confirmed in other studies using PAN nanofiber (Fig. 9b) [83]. Moreover, the integration of bead-on-string with other bead-free nanofibrous membranes has been indicated to provide better filtration performance than that of a single layer of beaded nanofiber (Fig. 9c) [84]. This kind of bilayer structure provides higher filtration efficiency and a lower pressure drop compared to the single-layer beaded membrane. This is due to the higher filter thickness and lower packing density at the same basic weight. Also, the combination of the beaded layer at the bottom and the bead-free layer at the top causes changes in the dominance different filtration mechanisms when the air passes through each layer. Diffusion efficiency is improved through the top, bead-free layer due to its high thickness and low packing density, and whereas the bottom layer with beads enhances the interception mechanism due to its smaller pore size. The bead-on-string structure was initially expected to generate high porosity and, consequently, low pressure drops. However, the high-pressure drop provided by the beaded structure compared to its bead-free counterpart contradicts such a claim in other experimental studies [82]. The effect of the high packing density of the beaded structure is the main reason for this apparent discrepancy.

Despite the numerous publications on mechanical air filtration [11], it is still challenging to assert that mechanical filtration alone is not adequate to achieve high filtration efficiency for PM < 0.3 without scarfing the pressure drop and quality factor [85]. Managing and enhancing the internal structure of the filter, including features such as pore size, porosity, nanofiber diameter, and membrane thickness,

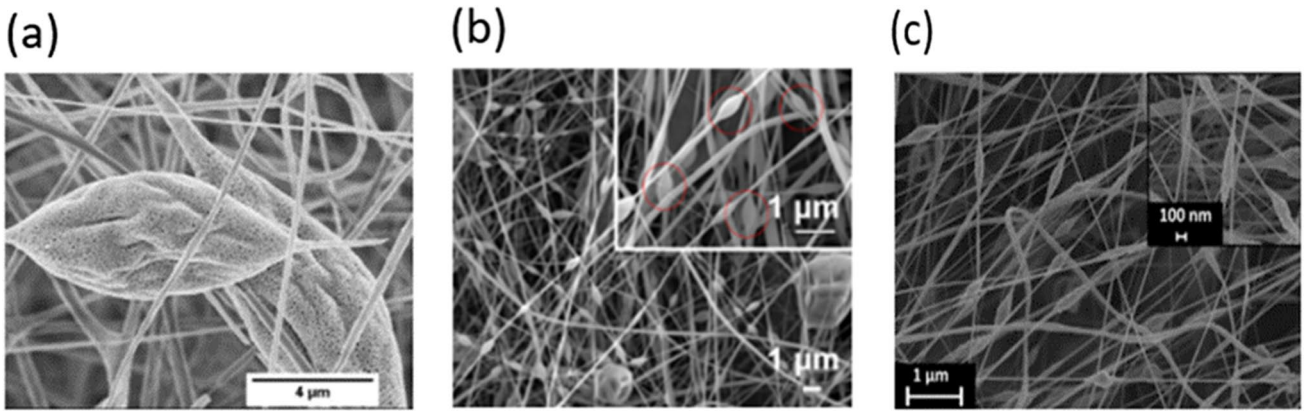

Fig. 9 Bead-on-string polymer nanofiber: **a** PLA (Reproduced with permission from [84], Copyright Elsevier, 2015) and **b** PAN (Reproduced with permission from [83], Copyright Elsevier, 2019)

provides the possibility to engineer high-performance air filters [86]. Those parameters remain crucial design factors in air filters which attract considerable research attention due to their significant impact on the overall structure and performance of a filter. Furthermore, many studies of mechanical air filtration concentrate on collection efficiency and the pressure drop associated with clean filter materials during a stable phase. However, these studies offer limited insights when it comes to achieving higher efficiency and in the development of ultra-low particulate air filters. Only a few studies have addressed the long-term unsteady filtering process during mechanical filtration, which is crucial for prolonged periods of filtration [87, 88]. Researchers have recently focused on the necessity for additional filtration mechanisms to complement mechanical filtration, particularly for the filtration of small PM. One air purification mechanism that has shown great promise in achieving higher efficiency while maintaining lower pressure drops and enhanced long-term performance is electrostatic filtration [21, 22, 89, 90].

3 Electrostatic filtration

3.1 Experimental work related to electrostatic filtration

Electrostatic capture filtration refers to the gathering of aerosol particles or pathogens within an electric field generated by the image force, charged coulomb force, and electric polarization [91]. Several studies have investigated factors influencing the purification capabilities of air filtration materials [92], and a recent study demonstrated advances in triboelectric nanogenerator (TENG) air filters in attaining high PM removal efficiency [93]. These self-charging filters consist of polytetrafluoroethylene (PTFE) modified with silica nanoparticles (NPs) and a core–shell nanofiber made of polypropylene and polyethylene (PP/PE). During the spinning process, the composite membrane becomes bipolarly charged in situ due to the triboelectric effect within the nanofiber matrix, and this significantly enhances the removal efficiency of PM up to 99.28% with a pressure drop of 26.46 Pa and quality factor of 0.19 Pa^{-1}. A novel switch-based air filter has also been developed which is characterized by high transparency, the efficient removal of PM, and low air resistance [94]. This innovative filter utilizes a transparent nylon/chitosan nanofiber, which at a high airflow velocity of 1 m/s and with an applied voltage of 200 V achieved a filtration efficiency of 95% for PM2.5 particles. The unique feature of this filter is its ability to function as a standard PM filter for low PM concentrations when in the OFF condition (DC field). Additionally, the filter membrane exhibits multifunctional properties beyond mere filtration. It exhibits high antibacterial activity and has the capability to adsorb substances such as ammonia and formaldehyde. Another novel approach has been used to introduce durable and highly efficient face masks featuring a multi-structured PLA [95]. The design is distinctive due to the fabrication of electrospun fibrous membranes with an average nanofiber diameter of 130 nm which serve as the filter media. The hydrophobic PLA is spun into a biodegradable nonwoven PLA fabric with varying degrees of alignment, ranging from random to highly symmetrical arrangements. The entire structure shows high durability and tensile strength and remarkable electrostatic filtration efficiency even in the presence of moisture. Meanwhile, a fully biodegradable piezoelectric membrane has been developed using polyvinyl alcohol (PVA) and glycine (GLY) via the electrospinning process [96]. The precise control of process parameters ensures that the glycine crystallizes into a highly piezoelectric β-phase during electrospinning, enabling the filter membrane's piezoelectric responses. Face masks created from the PVA-GLY membrane exhibited exceptional and stable filtration efficiency of 97% over 6 h of continuous filtration at high concentrations of PM0.3. Furthermore, in terms of biodegradability, the PVA-GLY masks were completely broken down within a few weeks. PLA and cyclodextrin (CD)/PLA nanofibers have also been manufactured via electrospinning and employed for the filtration of PM and volatile organic compounds (VOCs) [97], and it has been shown that the most effective air filter was 2.5 wt% CD/PLA, which displayed the highest filtration efficiencies in achieving 96% and 99% capture of PM2.5 and PM10, respectively (Fig. 10). This enhanced performance was attributed to the higher nanofiber surface area and porosity compared to pure PLA. Moreover, the optimum ratio of 2.5 wt% CD/PLA demonstrated superior VOC entrapment, indicating the high efficiency and rapid entrapment of volatile compounds. In addition, the 2.5 wt% CD/PLA-based triboelectric nanogenerator exhibited the most significant electrical signals, reaching 245 V and 84.70 μA which represent a threefold enhancement in electrical output compared to pure PLA compositions. These findings suggest that the 2.5 wt% CD/PLLA nanofiber can elevate surface charge density, thus facilitating enhanced PM capture via electrostatic interaction (Fig. 10).

3.2 Mechanism of electrostatic filtration

Electrostatic filtration mechanisms operate based on the interaction of the electrostatic charges between particles and the filtering media. Two primary types of electrostatic force are involved in the capture of PM: coulombic and dielectrophoretic forces [98]. The nature of these forces depends on the charged states of the nanofiber and the particles. When particles and nanofiber possess unipolar or bipolar charges,

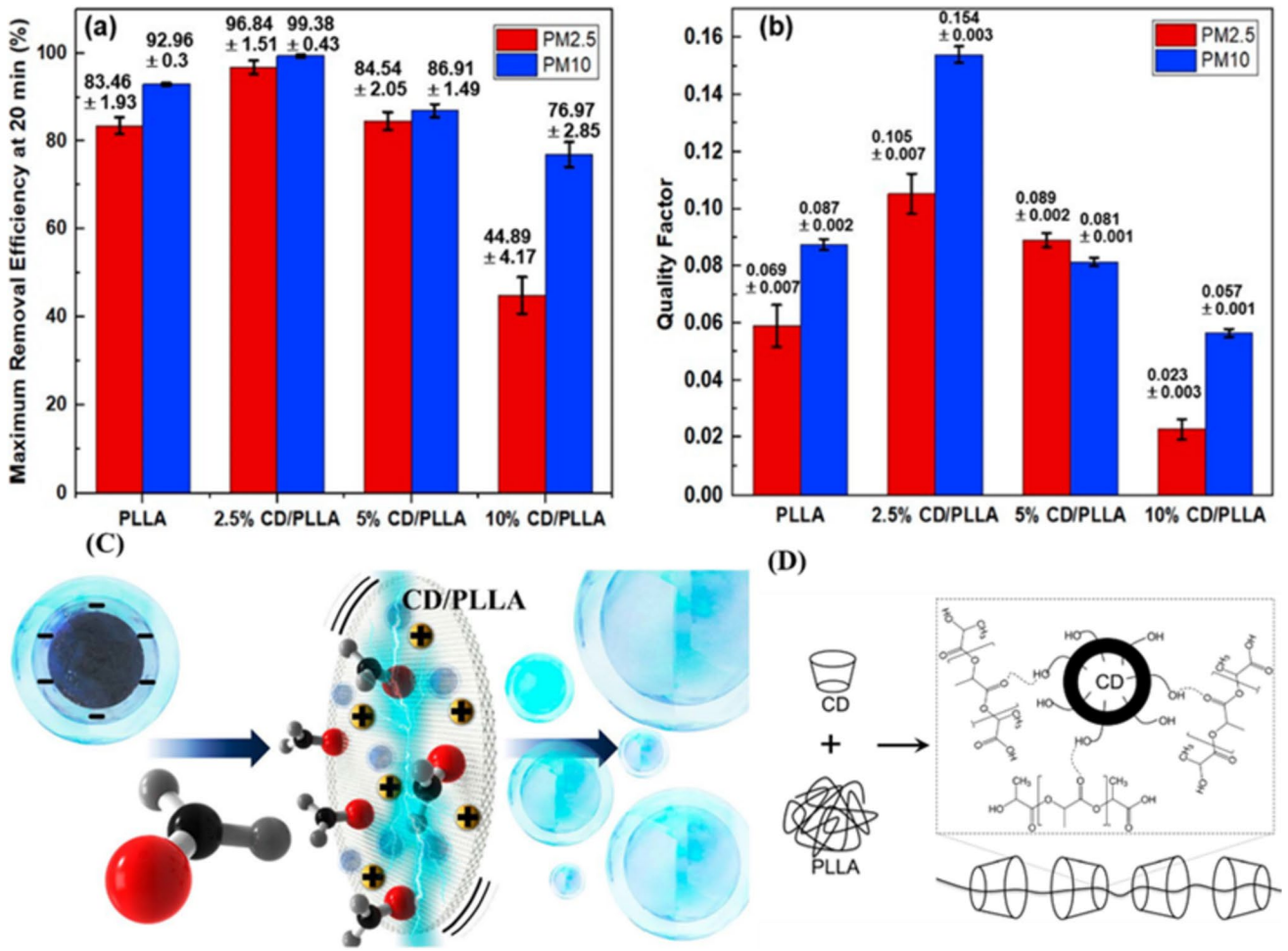

Fig. 10 Removal efficiency of PM2.5 and PM10 (**a**), quality factor of CD/PLLA nanofiber at different CD concentrations (**b**), electrostatic filtration mechanism through the CD/PLA nanofiber membrane (**C**), and schematic drawing for the chemical interaction between CD and PLA molecular chains [97] (Open access)

they attract each other through coulombic forces. In cases where either the particles or the nanofiber are in a neutral state, charging one polarizes the other, leading to attraction via dielectrophoretic forces. One crucial aspect of the electrostatic mechanism is that it does not affect the airflow, allowing for enhanced filtration efficiency without reducing air permeability. However, despite numerous theoretical models proposed for electrostatic filtration, the accurate prediction of capture behavior via electrostatic attraction remains challenging due to the complexity involved in quantifying charge distributions at microscopic levels. Nevertheless, the dielectric constants of the nanofiber and particles play significant roles in determining charge distribution and particle capture efficiency in electrostatic mechanisms [99].

For particles below 0.2 μm in size, all physical filtration mechanisms are relatively inefficient. Therefore, the application of electrostatic forces in these cases can enhance the collection efficiency of fibrous filters. Electrostatic filtration occurs when the particles and nanofiber are of opposite charge, causing electrostatic attraction or coulombic force between them [100] which leads to the electrostatic deposition of particles on the nanofiber surface (Fig. 3b) [101].

The single-fiber efficiency of the coulombic force caused by a uniformly electret-charged nanofiber is given by [102]

$$\eta_C = \frac{nqQC_c}{3\pi^2\varepsilon_0\mu d_p d_f u} \tag{6}$$

where Q is the charge on a nanofiber per length unit (coulomb/m), q is the particle charge (C), n is the number of elementary charges on each particle, C_c is the Cunningham slip correction factor, ε_0 is the permittivity of free space (8.854×10^{-12} F/m), u is the air velocity (m.s^{-1}), μ represents the viscosity of air, and d_p and d_f are the diameters (m) of the particle and nanofiber, respectively. The intensity of the electric field denoted as E (V/m) may be determined

by a theoretical simplification assuming that the fiber can be treated as a uniformly shaped cylinder, particularly in the case where it is monopolar charged and possesses a net charge [103, 104], then

$$E = \frac{Q}{\pi \varepsilon_0 d_f} \tag{7}$$

Therefore, Eq. 6 can be expressed as a function of coulombic force and Stokes drag force ($F\mathrm{d} = 3\pi\mu \mathrm{d_p u}$) [103]:

$$\eta_c = \frac{E}{F_d} nqC_c \tag{8}$$

The first electrical air filter, which was introduced by Hansen in 1930 [105], applied this method. The filter employed charged particles of resin scattered over the surface of a fibrous wool pad. Due to frictional charging during the manufacturing process, the highly charged resin particles could attract dust particles due to electrostatic forces. These particles can maintain long-lasting electret charging due to the high electrical resistivity of epoxy. Similar to diffusion, the electrostatic filtration rate is enhanced at low face velocity and small particle size [106]. These provide small values of inertia and long residence times for particles to be attracted to the fibrous filter [107]. One of the obvious advantages of the application of electrostatic filtration over other mechanical filtration mechanisms is its large contribution to total filtration efficiency while still maintaining a low pressure drop [108–110].

3.3 Theoretical work related to electrostatic filtration

Several theoretical analyses have recently been reported which focus on deepening our understanding of electrostatic filtration mechanisms or seeking to improve the efficiency of electrostatic filtration through specific alterations in membrane design. A simulation study based on lattice Boltzmann combined with a discrete element method (DEM) was employed to simulate the transport and deposition of particles through virtual 3D electret filters [111]. The study compared polyvinyl chloride (PVC), polyacrylonitrile (PAN), polycarbonate (PC), and polyethyleneimine (PEI) in terms of their filtration performance and long-term stability. The computational data supported the experimental results which showed better outcomes for the PVC electret filter, followed by PAN, PC, and PEI. The study highlighted the fact that the dielectric properties of polymer materials significantly shape the interaction between particles and nanofiber surfaces, as well as the charge storage abilities of electrospun electret filters. It was observed that a higher polymer permittivity resulted in larger adhesion energy between PM and nanofiber, leading to an increase in charge density and subsequently better PM collection performance. This reflects the influential role of polymer permittivity in shaping the effectiveness of these electret filters in capturing particulate matter. Another computational modeling technique was designed to simulate the 3D mixed structure of polyurethane (PU) electrospun fibrous media embedded with polystyrene (PS) filler within their matrix [112]. The model took into consideration various inputs such as nanofiber diameter, accumulation velocity, basis weight, and the bending properties of the nanofiber in the presence of PS spacer particles. The morphological structure of electrospun nanofiber was also utilized to obtain higher filtration efficiency for aerosol particles within a diameter range of 20 nm to 5 μm at a face velocity of 10 cm/s. The results suggested that the incorporation of spacer particles into a fibrous filter can significantly both improve its filtration efficiency and reduce the pressure drop. A micro-electrostatic filter featuring a novel cylindrical structure has also been designed numerically to combat indoor pathogenic microbial aerosol pollution [113]. Simulation results comparing the new cylindrical filter and a conventional plate filter indicated that the cylindrical structure outperformed the electrostatic filter under various conditions. For instance, at air velocities ranging from 1.5 to 2.5 m/s, the filtration performance of the cylindrical membrane filter for PM0.1 particles was approximately 20 to 30% higher than that of the plate structure, reaching a maximum value of 29.76%. Furthermore, the pressure drop with the cylindrical micro-electrostatic structure was determined to be only half that with the combined plate-type conventional filter, suggesting significant energy-saving potential associated with the cartridge structure. The quality factor further demonstrated the superior filtration performance of the cylindrical filter, proving that the implementation of cylindrical micro-electrostatic filters in HVAC systems may be able to enhance indoor air quality and reduce the health risks associated with pathogenic aerosols.

Computational models have been employed to determine the effects of coulombic forces on the filtration efficiency of aerosol particles [114]. A software-coupling method was developed to create a 3D random nanofiber model to describe the microstructure of fibrous filters, and models encompassing flow, particle behavior, and the electric field were established which assumed uniform nanofiber potential and neglected the non-uniformity of particle charge distribution. The study investigated variations in filtration efficiency and pressure drop based on influential factors such as nanofiber diameter and potential, particle charge-to-mass ratio (Q/M ratio), solid volume fraction (SVF), and face velocity. The results indicated that filtration efficiency increased with particle size but was notably influenced by the particle Q/M ratio. The scale of the pressure drop exhibited an almost linear increase with SVF, while high SVF did not significantly enhance filtration efficiency for particles.

Additionally, the use of nanofibers of smaller diameter resulted in greater filtration efficiency.

3.4 Efficiency of electrostatic filtration

As discussed in Sect. 2.4, mechanical filtration depends mainly on the porous structure of the nanofibrous membrane. Increases in filter thickness, packing density, and basic weight, and reductions in pore size are commonly employed to attain high filtration efficiency. However, the breathability associated with the pressure drop of filter media may be sacrificed. This is an inevitable phenomenon with mechanical filtration. Despite efforts to modify the structure of nanofibrous membranes to alleviate the conflict between filtration efficiency and breathability, improvements in the quality factor of nanofibrous membranes have been still controversial. Therefore, the application of electrostatic filtration to fabricate electret membranes in this case may be more effective due to its distinct filtration mechanism [115]. Electrostatic filtration provides an active filtration mechanism compared to the passive nature of mechanical filtration, with electrostatic force based on coulombic interaction and an induced polarization that can effectively capture particles in a large attraction distance due to intermolecular electrostatic interaction [116]. This filtration mechanism is not dependent upon aspects of filter structure such as thickness or packing density, and hence, its use does not negatively affect the breathability of filter media [117] (Fig. 11). Electrostatic can be applied on fabricating electret membranes by using temporary charging methods, for example corona charging and in situ charging, or constant charging with triboelectric [118] or piezoelectric nanogenerators [119].

3.4.1 Pre-charged electret air filters

Electret filters can generate a quasi-permanent electric field when electrically activated, hence generating electrostatic force to capture particles. Electrical activation can be accomplished by embedding external charges for corona charging or aligning electric dipoles within electret materials for in situ charging. Surface potential and its stability over time reflect the electrostatic performance of electret membranes, and these indicators vary between different electret polymers and processing methods. Therefore, researchers have focused on improving the processes involved and finding suitable electret polymers in order to attain high surface potential with stable electrostatic filtration performance.

Corona charging In corona charging, a high voltage is employed to provide an external electrical field between asymmetric electrodes such as a point/wire and a plate/cylinder [120]. This electrical field generates corona charges through air ionization according to the intensity of the electric field. These corona charges are then embedded in the nanofiber through contact media by aerodynamic force and/or the surrounding ionized air. The first media can be achieved by applying corona charges before the solidification of the nanofiber, where charging is not affected by

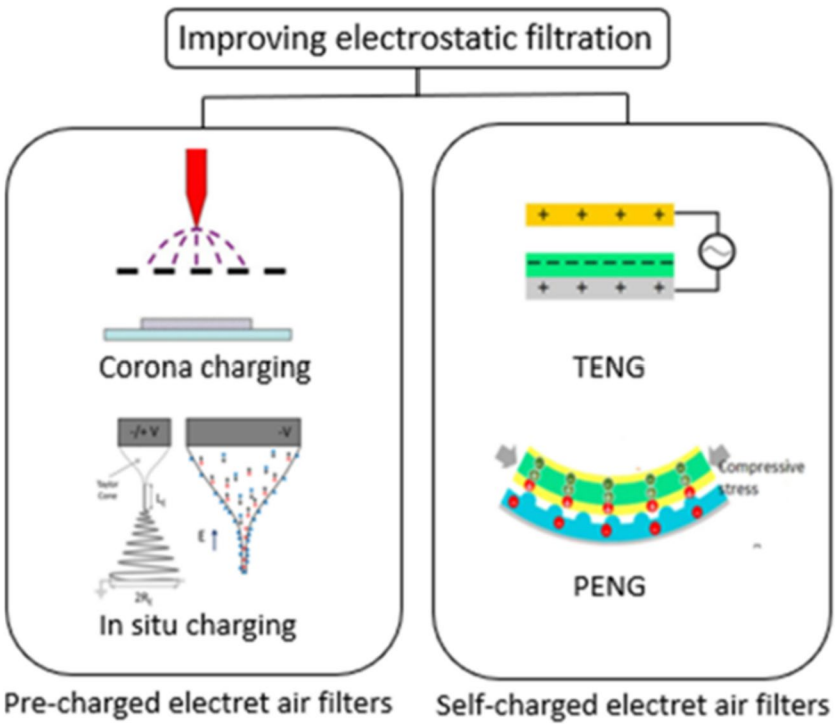

Fig. 11 Recent advances in electrostatic air filtration

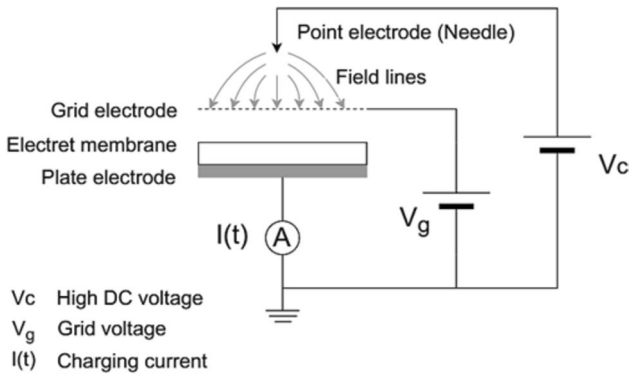

Fig. 12 Schematic diagram of a corona triode setup for electrostatic charging electret membranes

filter thickness. In the second media, charges are applied directly to the fibrous membrane (solidified nanofiber), and the distribution of charges depends on filter thickness [121]. Figure 12 shows a schematic of a common corona charging setup used in the electrostatic charging of electret membranes. The high voltage creates a strong electrical field around the point electrode, ionizing the air, and subsequently creating ions. These ions are accelerated by the electrical field and collide with the electret membrane, resulting in the generation of its surface potential. The insertion of an additional grid electrode allows the control of surface potential and charge uniformity. Therefore, this three-electrode system is called a corona triode [122]. Corona charging is generally considered to be a simple method to provide electrostatic filtration for commercial electret filters and has been commonly applied in this field. However, the retention of charge stored in dielectric materials is a main drawback of this charging technology, since the charge can easily dissipate in conditions of high humidity [123, 124].

Tabti et al. [125] under optimal conditions, the resulting surface charge density reached approximately 26 μC/m2, but exhibited rapid decline in less than 30 min. Additionally, elevating the temperature to 75 °C was observed to induce a charge dissipation of 20% within the same 30-min timeframe. Meanwhile, combining a DC with a pulse in corona charging provides a higher charge density compared to the use of DC or pulse charging alone, as indicated by Nifuku et al. [126]. These authors also claimed that adding SiO_2 and TiO_2 as charge enhancers improved the surface charge density, resulting in the high filtration efficiency of PP filters (99.32%). The improvement of the electret property of fibrous polymer filters by embedding charge enhancer particles was also addressed by Zhang et al. [124]. Here, the addition of magnesium stearate (MgSt) to electret nonwoven PP membranes modified the crystal structure of the nanofiber, hence improving its electret properties and, consequently, the filtration performance of the fibrous filters, giving filtration efficiency of 97.96%, a low pressure drop of 84.28 Pa, and a high quality factor (QF) of 0.046 Pa^{-1} after corona charging (Fig. 13a). Similarly, Kulmala et al. [37] showed how the filtration efficiency of normal medical face masks can be significantly improved by applying corona discharging for particles provided by a simple battery-operated charger (Fig. 13b).

However, along with the use of nanofibers to obtain higher filtration performance in air filtration applications, and especially in medical face masks, electrospinning has been employed to fabricate electret nanofibers by controlling the voltage applied and charging distance. Sun and Leung [127] applied corona discharge for their PVDF nanofibrous electret filters with a nanofiber diameter < 500 nm and found that a high surface potential of 115.2 V was obtained by using a high charging voltage of 20 kV and a short charging distance of 30 mm. This was due to the higher rate of ionization of air molecules, resulting in more ions deposited onto the surface of the filters [125, 128]. Moreover, this study used multiple-layer filters with lower nanofiber density, which could provide higher efficiency for both mechanical and electrostatic filtration as well as a smaller pressure drop compared to single-layer filters with high nanofiber density (Fig. 14a). In terms of mechanical filtration, stacking up multiple layers provided sufficient space for the aerosol flow to slow down as it collided with the upstream face of each layer. This reduction in the speed of the particles benefitted the diffusion mechanism, hence increasing mechanical filtration efficiency. Furthermore, the use of multiple layers with low nanofiber density resulted in higher porosity, which consequently led to a lower pressure drop. In electrostatic filtration, the stacking of multiple layers benefitted charge efficiency due to the existence of less interference between adjacent nanofibers compared to the situation with a single layer and denser nanofiber, consequently leading to higher electrostatic filtration efficiency. The achievement of high performance in filtering airborne novel coronavirus (COVID-19) and nano-aerosols by reducing filter basis weight and stacking more filter layers was further investigated in subsequent research [62] which also addressed the effect of nanofiber diameter on filtration performance. Nanofibers with smaller diameter provided improved mechanical filtration, including by diffusion and interception, and a modest improvement in electrostatic capture. The significant improvement in filtration performance was due to the higher charge density acquired by smaller nanofibers, hence inducing a stronger dipole moment to attract more neutral PM as it approached the charged nanofiber. This dielectrophoretic interaction also provided better filtration performance for the electret nanofiber compared to uncharged counterparts (Fig. 14b).

In situ charging by electrospinning In situ charging is a method that applies charges so as to align the dipoles of

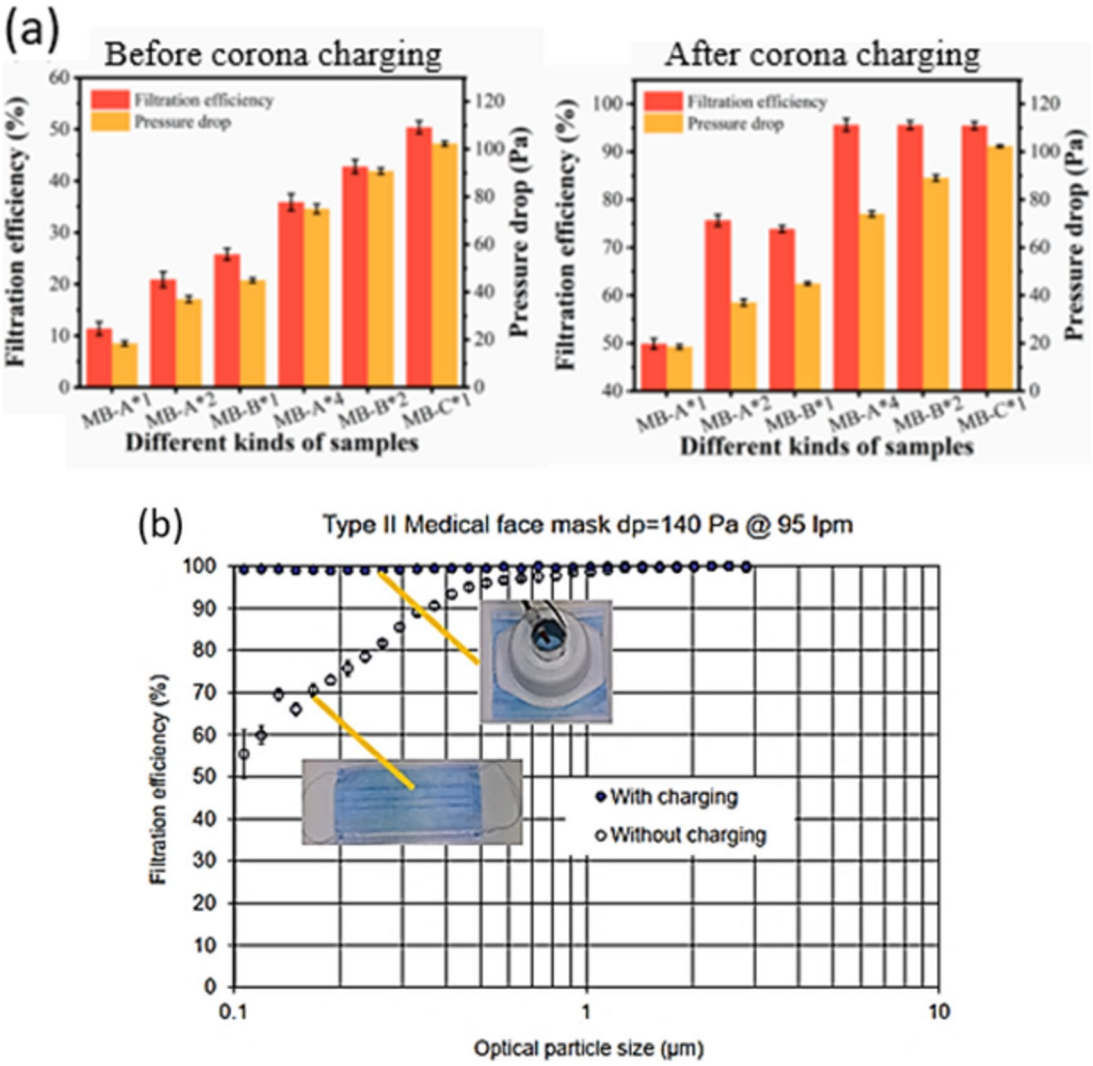

Fig. 13 The role of corona charging in improving filtration performance of melt-blown fibrous filters: **a** PP/MgSt melt-blown nanofiber [124] (Open access) and **b** type II face masks in normal conditions and with particle charging [37] (Open access)

polymer solutions in which their molecular bonds are loose. Fiber spinning is driven by electrostatic force and the use of polarized nanofiber which is subsequently produced after solvent evaporation. Therefore, the spinning and charging of the nanofiber can be combined in one process. The most common type of in situ charging process is electrospinning. Due to the principle of in situ charging, the electrostatic filtration performance of electret nanofibrous membranes strongly depends on the dipole moment and subsequently surface potential, which varies between different electret polymers due to differences in their chemical structures. One study has investigated the filtration efficiency of different electret polymer membranes, including PAN, polyvinylpyrrolidone (PVP), PS, and PVA, taking into consideration the effect of their different dipole moments [129]. The results indicate that the best PM capture (> 99%) was exhibited by the PAN nanofiber due to its dipole moment (3.6 D) being higher than those of the other materials.

Similarly, Li et al. [130] have demonstrated the importance of polarity or dipole moment in affecting the filtration efficiency of polymer nanofibrous membranes, which is due to the electrostatic interaction between the charged nanofiber and particles. PC exhibited the highest percentage PM removal compared to PVA and PS membranes owing to its higher dipole moment. Additionally, reduced nanofiber diameter as well as increased membrane thickness also improved mechanical filtration, hence contributing to the overall enhancement of filtration by the PC nanofibrous filter and the combination of high surface area (mechanical filtration) and high polarity (electrostatic filtration) provided a PC nanofibrous membrane with close to 100% filtration efficiency. Liu et al. [131] have used similar adaptations to

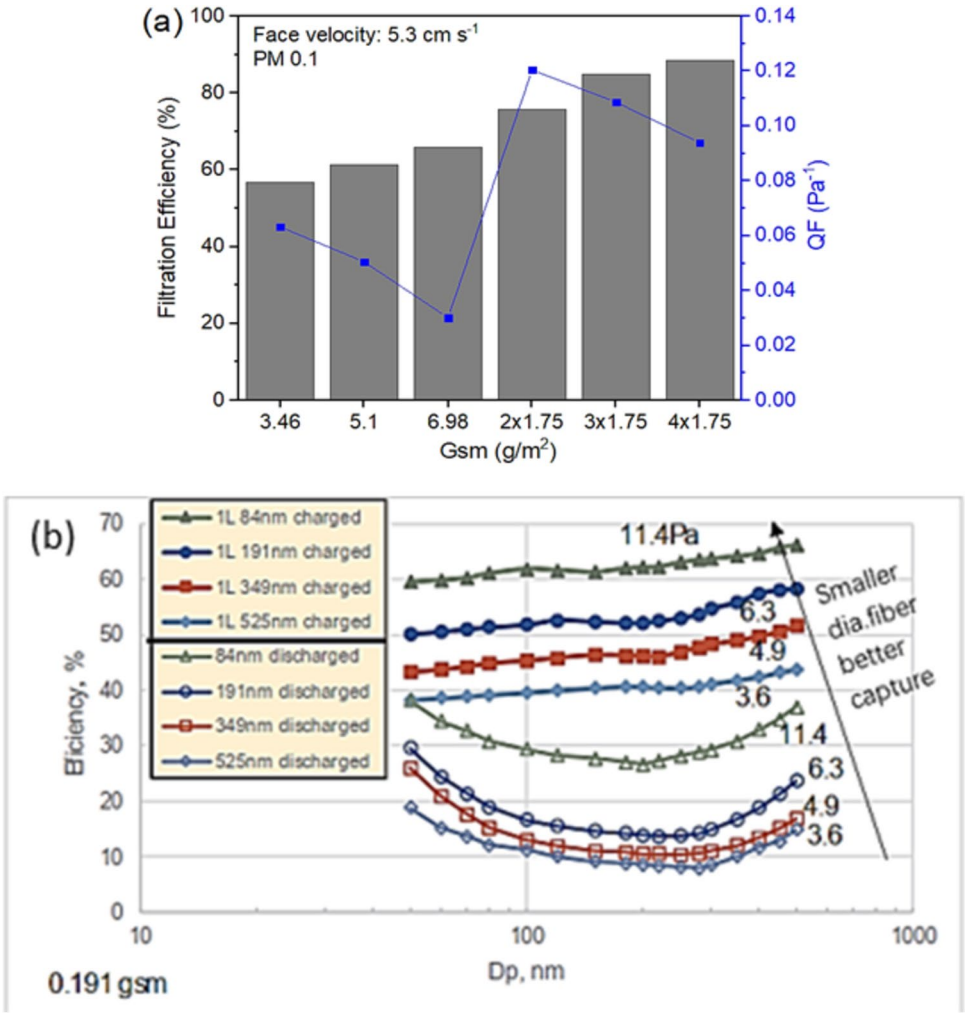

Fig. 14 Electret nanofibrous membrane with corona charging fabricated by electrospinning: **a** effect of filter weight density and number of layers [127] (Open access) and **b** effect of nanofiber size on filtration performance [62] (Open access)

produce high-performance PM0.3 air filters using PVDF nanofibrous membranes. They applied an electret electrospinning/netting technique to fabricate PVDF nanofiber/nets in which interlinked 1D ultrafine nanowires (~ 21 nm) were distributed between scaffold nanofiber. This structure provided small pore sizes and a high surface area for the membranes, hence improving mechanical filtration efficiency. Also, the nanonets exhibited a higher degree of self-polarization or dipole arrangement under high-voltage charge compared to simple nanofiber structures. Consequently, a greater level of transformation from the nonpolar α-phase to the strongly polar β-phase was triggered which, in turn, increased the spontaneous polarization per unit cell in the nanonet structure. This resulted in the high surface charge density and larger dipole moment of the PVDF nanonets, which subsequently possessed a surface potential (6.8 kV) double that of the PVDF nanofiber. Such a high surface potential of the PVDF nanofiber/nets combined with low packing density also led to better filtration performance in terms of both efficiency and pressure drop compared to those of PAN, PA6, and PU counterparts. Furthermore, the ferroelectricity property of polymers provided a self-polarization effect for the electrospun polymer nanofiber, resulting in good filtration performance of electret membranes such as Nylon 11 [132]. Other similar research on oriented dipole electret filters using polymer nanofibers of material such as polybenzimidazole (PBI) [133] and PU [134] has also highlighted the important role of the dipole moment of the nanofibrous membranes in enhancing electrostatic filtration.

However, in situ charging using electrospinning to fabricate electret membranes also has the major disadvantage of rapid charge dissipation [135], as with corona charging. Therefore, the addition of NPs as charge storage enhancers is required to enhance charge stability. For example, X. Li et al. found that, when doped with silica (SiO_2) NPs with permanent dipole orientation, polyetherimide (PEI) electrospun nanofiber can maintain high stability in the surface potential of the electret membrane over long periods (Fig. 15a) [136]. This study doped PEI electrospun nanofiber with different NPs, including SiO2, Si3N4, BaTiO3, and boehmite. The PEI/SiO2 nanofibrous filter exhibited excellent filtration performance compared to the other composite filtering media,

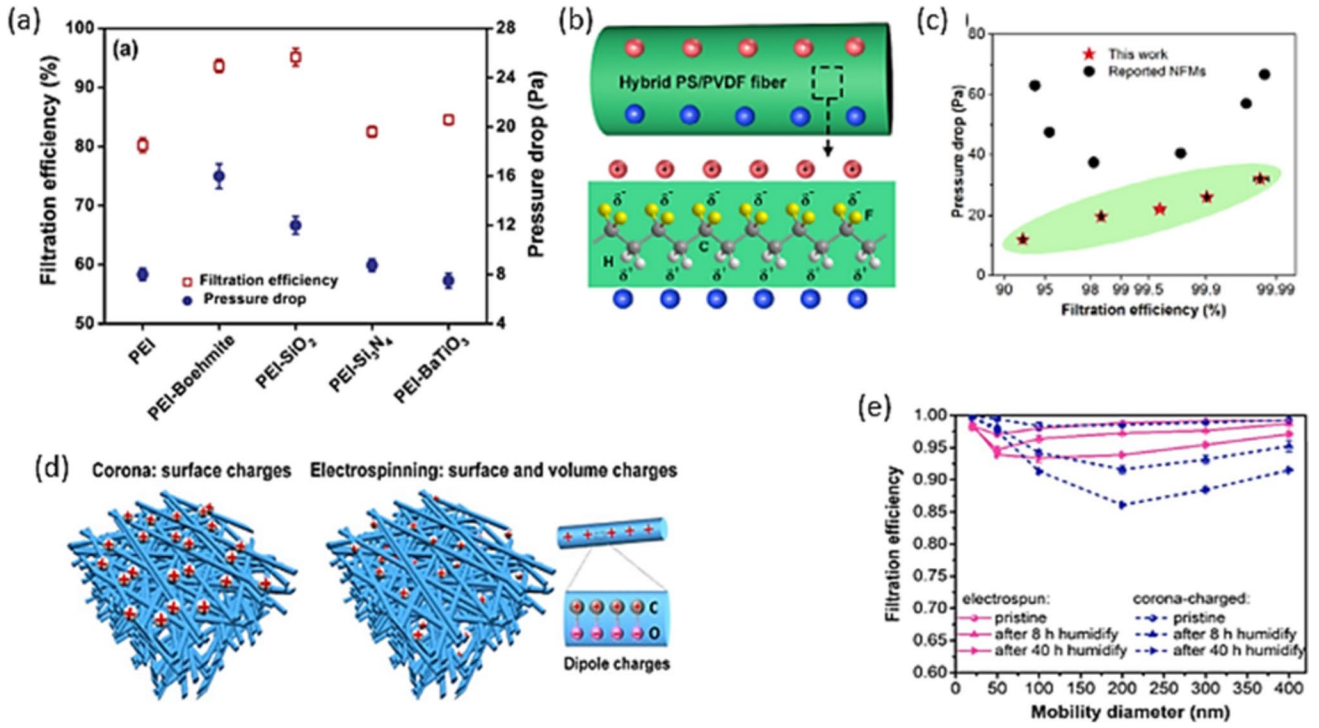

Fig. 15 In situ charging for electret nanofibrous filters: **a** Filtration performance of different NPs electret PEI membranes [136]. **b** Schematic illustrating the contribution of PVDF on electret effect. **c** Comparison of filtration performances (Reproduced with permission from [137, 139–141] [138], Copyright Elsevier, 2020). **d** Schematic description of charge types in corona-charged and electrospun membranes. **e** Normalized surface potential decay of relevant hybrid membranes at room temperature (Reproduced with permission from [136], Copyright Elsevier, 2020)

with its best filtration properties at 99.992% and 61 Pa of FE and pressure drop, respectively. Meanwhile, other NPs such as PTFE enhance polarization when doped with PVDF nanofiber [137]. This is due to the abundant fluorocarbon segments with strong electronegativities in both PVDF and PTFE which increase the numbers of oriented dipoles under high-voltage charges. The interfacial polarization charges at the PVDF-PTFE interface also prevent decay in surface potential, hence maintaining high charge stability. Another possible adaptation is to create a hybrid electret nanofiber containing two different electret polymers. For example, Y. Li et al. [138] attempted to improve the electret effect by creating a dual-system charge within nanofiber of PS/PVDF, exploiting their complementary dielectric properties. The distinct electronic transport capabilities between PS and PVDF accumulated charges at their interface zone and hindered them from transferring the PM (Fig. 15b). The hybrid PS/PVDF nanofibrous membrane exhibited better filtration efficiency (99.752%), low air resistance (72 Pa), and a long retention time compared to those found in related studies (Fig. 15c) [137, 139–141]. In addition, in situ charging using electrospinning has been found to provide longer charge retention times and better stability of filtration performance compared to corona charging due to the surface charges generated during the process (Fig. 15d, e) [142].

3.4.2 Self-charged electret air filters

As discussed above, both corona charging and electrospinning are temporary charging methods to apply electrostatic filtration for nanofibrous membranes. Although the charge stability of an electret filter can be improved by using advanced processes, electret materials, or doping with NPs as charge enhancers, the dissipation of electrostatic charge over time is still inevitable [143]. Therefore, an electret membrane with a constant charge supply might be a solution to achieve stable electrostatic filtration. Recent studies have attempted to employ triboelectric nanogenerators (TENGs) and piezoelectric nanogenerators (PENGs) to harvest energy from human respiration and friction to recharge the filters and therefore to maintain the electrostatic filtration effects in electret membranes for longer [144–146].

TENGs were first introduced by Fan et al. [147] for potential application in harvesting energy from different sources such as human activity, mechanical vibration, and

ocean waves. Two polymer sheets with different triboelectric properties were stacked to generate charge due to friction between their surfaces when subjected to mechanical deformation. Recently, some researchers have focused on the application of TENGs for self-powered electret face masks [148–150]. Integrating TENGs into nanofibrous membranes in face masks can lead to the higher stability of surface potential, hence maintaining the high filtration performance of filters over time. A concept of self-powered electrostatic adsorption face mask (SEA-FM) proposed by Liu et al. [151] has shown high filtration efficiency (86.9% for ultrafine particles) (Fig. 16a) and stably remained for 240 min and a 30-day interval. The continuous supply of electrostatic charge resulted in the stable retention of the surface potential of the PVDF-ESNF membrane, while the surface potential of the membrane without R-TENG decayed over time (Fig. 16b). This face mask was based on a poly(vinylidene fluoride) electrospun nanofiber film (PVDF-ESNF) and a TENG driven by respiration (R-TENG) (Fig. 16c). Another design of a self-powered triboelectric face mask proposed by Ghatak et al. [152] used three stacking electret polymeric membranes (latex rubber-PU-latex rubber) as a TENG (TE) and one outer conductive layer (EL) (Fig. 16d). The mechanical deformation from different sources such as respiration, rubbing, or relevant facial gestures was able to produce sufficient charge to activate the electrocution layer (EL). The electrical field generated from these charges can provide sufficient electrocution to deactivate the exterior proteins of viral particles. In addition, a recent study of self-powered electret face masks using TENG has confirmed that electrospun PVDF/PS nanofibrous membranes (Fig. 16e) can not only attain a better filtering effect (> 95.3% PM from 0.3 to 10 μm) compared to PP melt-blown nonwoven filters in commercial masks (from 88.9%) (Fig. 16f) but were also recharged by the TENG provided from friction. Therefore, this kind of filter exhibits good recoverability of filtration performance along with a longer lifecycle.

PENGs were first proposed in 2006 [154] for the harvesting of energy employing piezoelectricity from nanoscale mechanical processes such as human motions. Owing to their many advantages, including small dimensions and simple structure and operation, PENGs have high potential in applications such as in power supply for portable electronic devices or self-powered systems [155]. The use of piezoelectric materials such as PVDF nanofiber to fabricate electret filters of face masks has recently become popular, and a multi-layer piezoelectric nanofibrous membrane could be employed as a PENG to provide a constant charge supply to maintain stable electrostatic filtration.

The integration of PENGs into face masks has been proven to generate sufficient energy to supply attached sensors or active antimicrobial devices. A hybrid piezoelectric nanogenerator (hPENG) based on a PVDF nanofibrous membrane was proposed by Mariello et al. [156] and has been integrated into surgical face masks as a wearable energy harvester (Fig. 17a). This nanogenerator is able to collect energy from both piezoelectricity and the triboelectricity generated by facial motions such as during the breathing cycle and when adjusting a mask, which induce deformation and friction (Fig. 17b). The strong electrostatic behavior of the membranes reflects the ultrasensitive mechanoelectrical transduction properties of this PENG. The operation of the device also exhibits high stability and resistance in wet and warm environments. Based on the operating principles of hybrid PENGs, Kang et al. [157] have demonstrated an electrostatic air filter membrane applied in face masks based on piezoelectric PVDF nanofiber stacked with nylon mesh substrates. The PVDF nanofiber-nylon mesh multilayer structure can fulfil the self-charging function of electret membranes from two power supplies: triboelectricity from the PVDF-nylon frictional contact and piezoelectricity from membrane deformation during human respiration (Fig. 17c). In other words, this structure can be considered a hybrid piezoelectric-triboelectric nanogenerator and as a self-charged electrostatic filter has shown remarkable filtration performance with a higher quality factor compared to discharged masks for various PM sizes (from 0.3 to 2.5 μm) regardless of the number of layers (Fig. 17d).

4 Antimicrobial filtration functionality

4.1 Experimental work

With the recent advances in filtration using nanofibers, as mentioned in Sects. 3.1 and 3.2, face masks and respirators can effectively capture ultrafine airborne and droplet-borne pathogens. However, aerosols containing viruses and bacteria captured inside filter membranes or on the outer layers of masks can result in self-inoculation, since mask filters provide no antimicrobial function. Pathogenic microbes such as the SARS-CoV-2 virus can remain infectious on mask surfaces for more than 6 days [158], hence making masks fomites and causing secondary transmission or cross-infection. Contact with infectious masks for even short periods can lead to the transfer of pathogenic microbes onto the

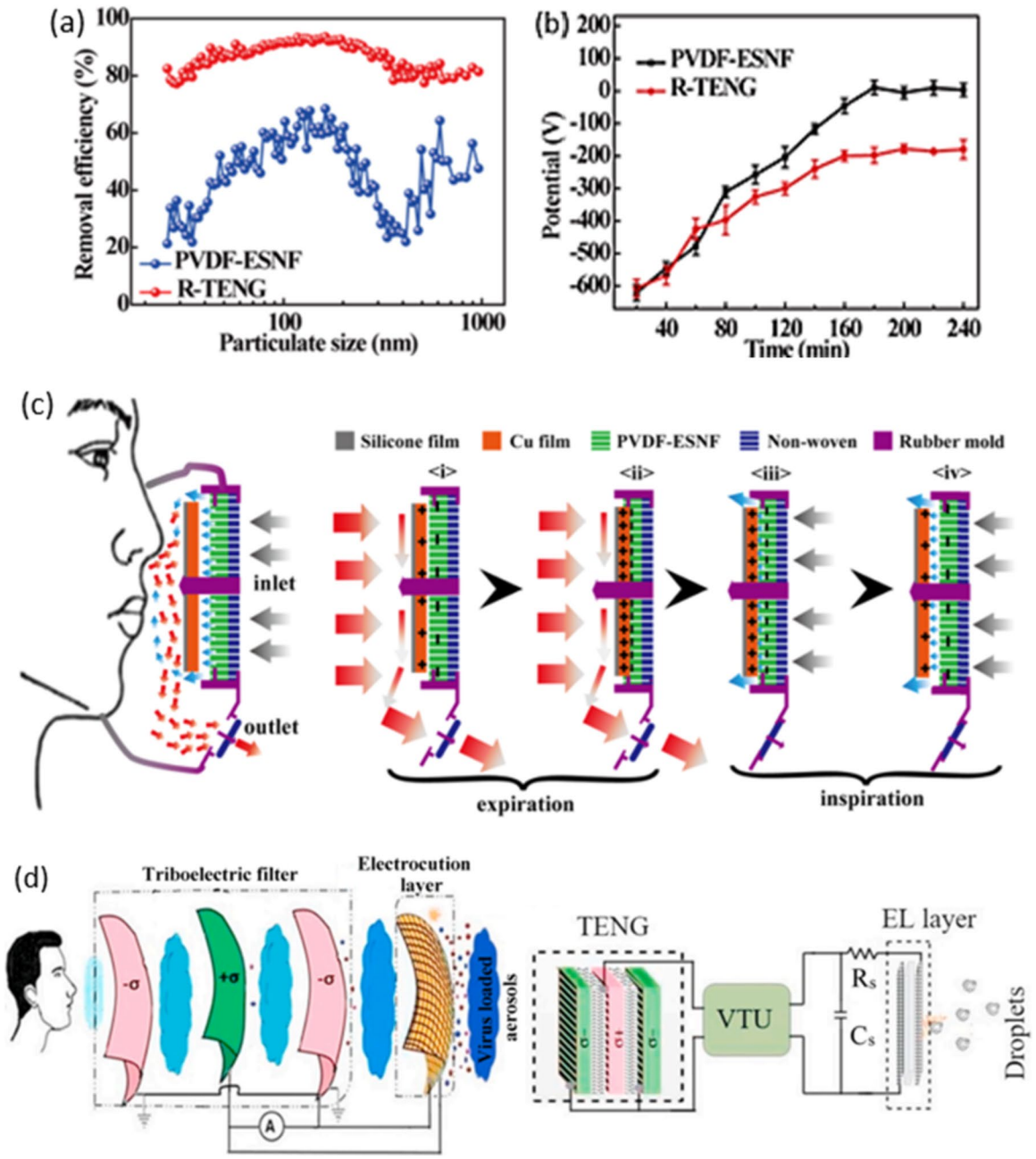

Fig. 16 Self-charged electret air filters by triboelectric nanogenerators: **a** Corresponding removal efficiency of the PVDF-ESNF and R-TENG. **b** Average surface potential change of the single PVDF-ESNF and the PVDF-ESNF implanted in the R-TENG in 240-min filtration. **c** Working principles of R-TENG self-powered face mask by periodic expiration and inspiration (Reproduced with permission from [151], Copyright American Chemical Society, 2018). **d** Schematic representation of the proposed triboelectric multilayers comprising self-powered mask. The inner three layers (from face side) act as TE filter, and the outer layer is the EL made with conducting mesh (Reproduced with permission from [152], Copyright Elsevier, 2021). **e** Schematic diagram of PVDF/PS electrospinning membranes preparation process. **f** The comparison of filtration performance between melt-blown PP nonwoven and electrospun PVDF/PS electret membrane (Reproduced with permission from [153], Copyright Elsevier, 2023)

hands, and, for example, 32% of influenza A viral cells present may be transferred within 5 s [159]. Therefore, the integration of an antimicrobial function into masks can enhance their lifecycle and reusability in addition to providing safer disposal and reducing contamination. Many antimicrobial agents have been applied via the doping of nanofiber, such as with metal-based NPs and organic compounds. This section reviews some common antimicrobial substances and explains their biocidal mechanisms.

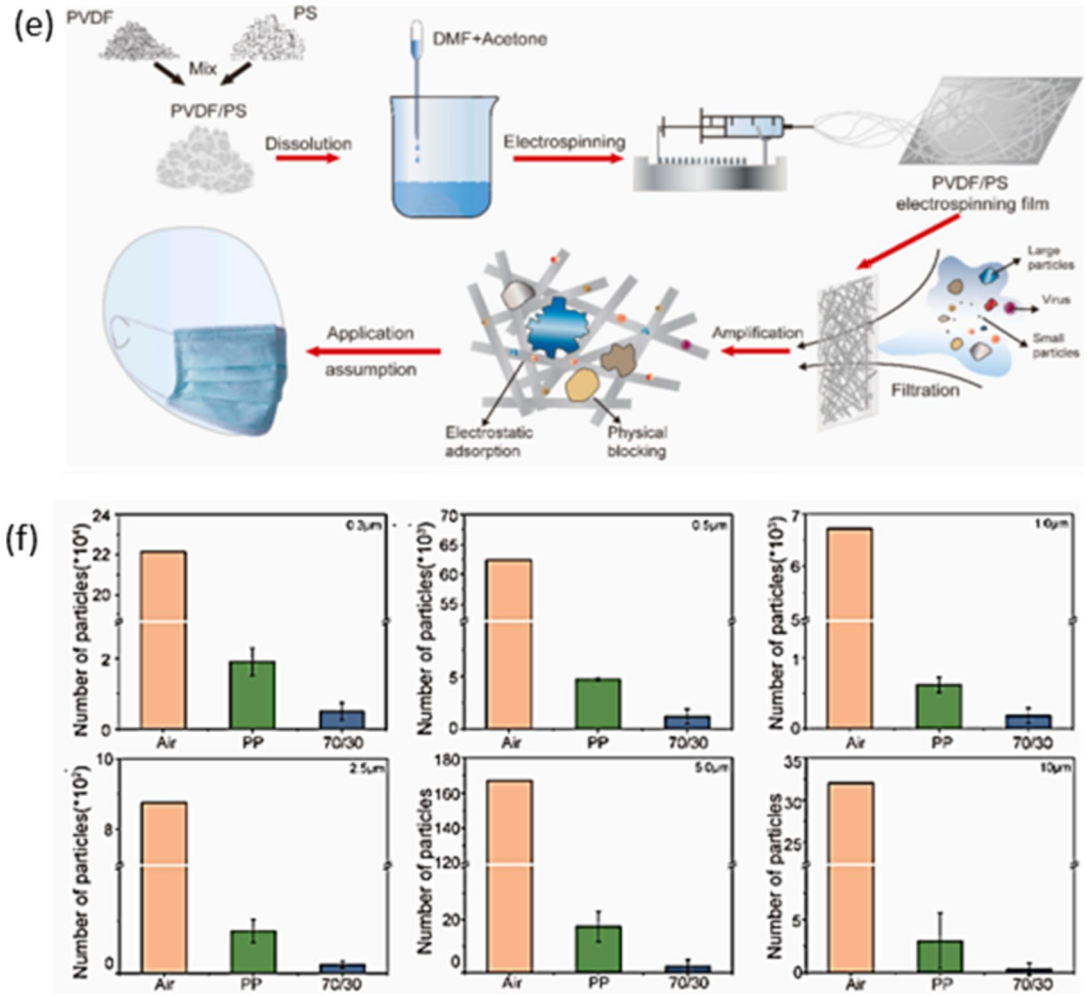

Fig. 16 (continued)

4.1.1 Metal-based NPs

Metal-based NPs have recently been applied to provide an antimicrobial function for mask filters owing to their physiochemical properties that can inactivate pathogens [160]. The biocidal function of metal-based NPs is based on four mechanisms: (i) by attachment to viruses and disrupting their penetration of host cells; (ii) where the metal ions damage microbial functions by binding and precipitating thiol groups (SH) in proteins, or phosphate groups (PO_4-) in deoxyribonucleic acid (DNA) and adenosine triphosphate (ATP); (iii) via photocatalytic activity which produces reactive oxygen species (ROS) causing oxidative stress to viruses and bacteria; and (iv) by activation of the immune response of infected cells against the virus. The antiviral mechanisms of some common metal-based NPs are shown in Fig. 18.

Gold NPs (Au-NPs) generate a blocking site to block viruses from penetrating into host cells and have been claimed to reduce measles virus infection by 92% after 6 h of interaction by inhibiting viral attachment to host cells [162]. Also, Au-NPs coated with mercaptoethyl sulfonate (Au-MES NPs) can efficiently block the penetration of herpes simplex virus type 1 (HSV-1) [163]. The advantages of using Au-NPs for antimicrobial activity include their stability, biocompatibility, and bioconjugation [164]. However, their application in antiviral face masks would be impractical due to their high cost.

In comparison with Au-NPs, silver (Ag) NPs cost less and have been widely applied as a powerful antimicrobial agent. Ag NPs, including those containing silver oxide (Ag_2O) and silver monoxide (AgO), exhibit broad-spectrum antimicrobial activity due to their ability to damage the SH groups of microbe proteins. Inactivation is the main biocidal mechanism of these antimicrobial substances [165], which have been widely applied in medical equipment, textiles, and wound dressing [166, 167]. Silver nanoparticle–based yarn produced by Yan et al. [168] exhibited antimicrobial activity against various bacteria such as *Bacillus*, *Staphylococcus*,

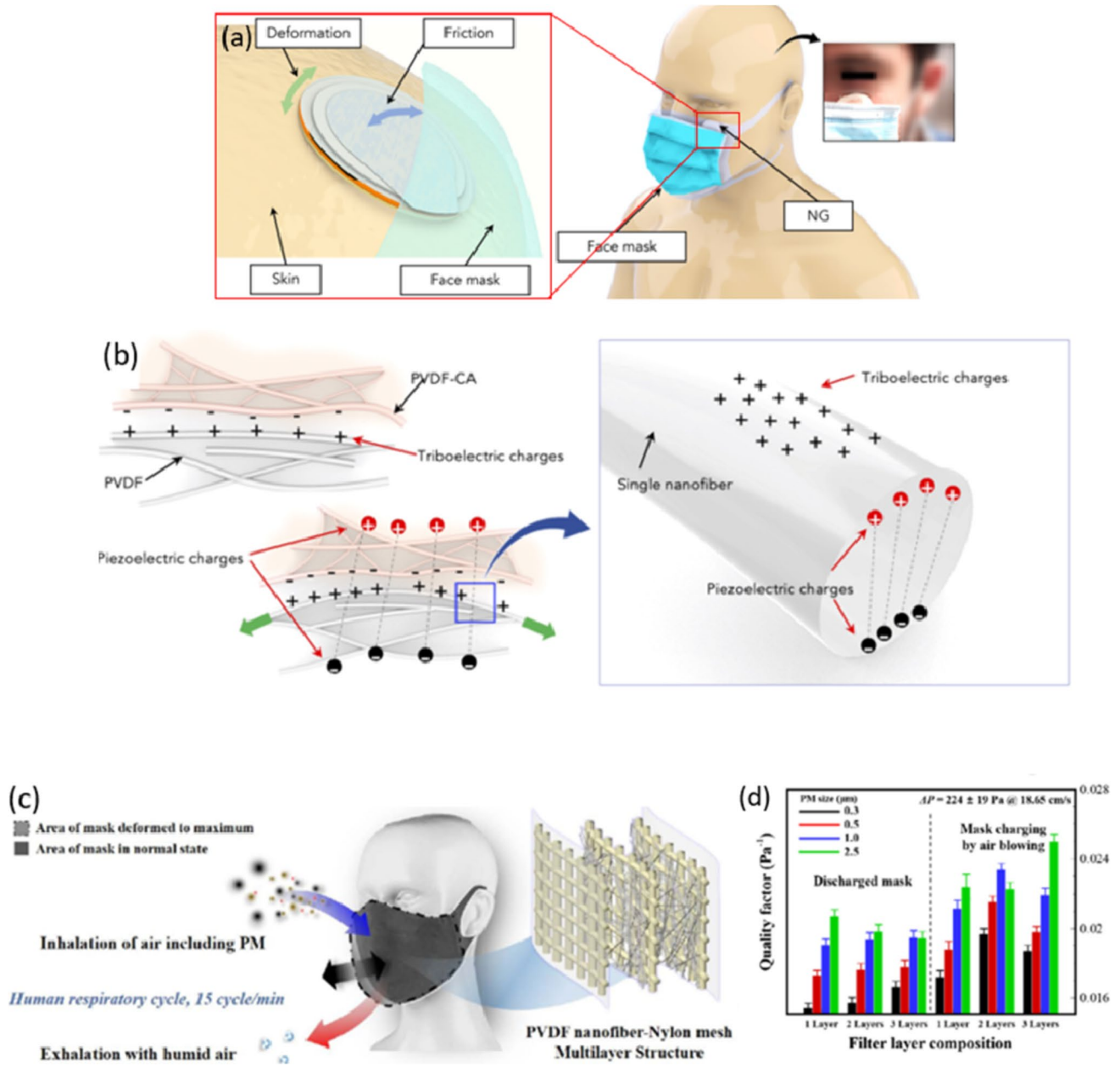

Fig. 17 Self-charged electret air filters by piezoelectric nanogenerators: **a** The applicability of the hybrid PENG underneath the surgical face mask. **b** Representation of the interactions between piezoelectric and triboelectric charges during the deformation of the composite electrospun bilayer (Reproduced with permission from [156], Copyright 2021 American Chemical Society). **c** Schematic for filter charging via bending and fluttering by air blowing, mimicking human respiration. **d** Quality factor comparison between mask charging by air blowing and discharged mask [157] (Open access)

Chlamydia, *Escherichia*, and *Pseudomonas*, and it maintained its effectiveness after being washed 100 times. Tang et al. [169] have found that silk nanofiber coated with Ag NPs exhibited significant antibacterial performance against *Escherichia coli* that similar to that of silver nanoparticle–treated wool fabrics [170]. The ion release rate of Ag NPs depends on their particle size, which can therefore affect their antimicrobial performance [171]. Some researchers have successfully fabricated Ag NPs with average particle sizes of 33 nm [172] and 7.1 nm [173], thereby providing much more efficient interaction with viruses due to their large specific surface area. One investigation by El-Sheekh et al. [174] used Ag_2O|AgO NPs with sizes ranging from 14.42 to 48.97 nm and achieved a 90% reduction in the cytopathic effect (CPE) of herpes simplex virus (HSV-1). Hiragond et al. [175] coated commercial face masks with

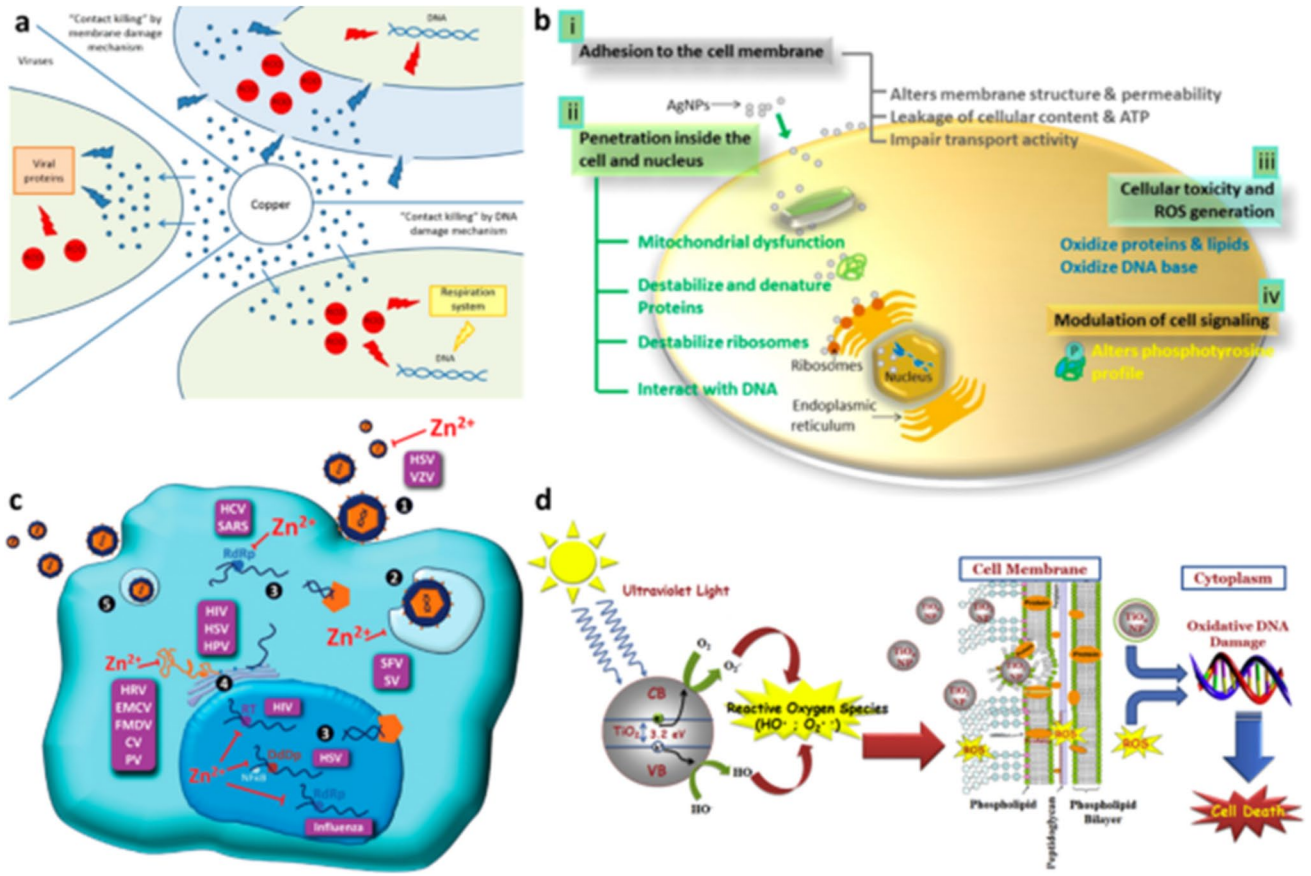

Fig. 18 Antiviral mechanisms of inorganic materials. **a** Antimicrobial contact killing mechanisms for copper include membrane degradation, genotoxicity, and potentially ROS. **b** Four prominent routes of antimicrobial action for silver include adhesions to cell membrane (i), penetration into cell and nucleus (ii), cellular toxicity and ROS generation (iii), and modulation of cell signaling (iv). **c** Actions of zinc throughout the cell and proposed mechanisms for antiviral properties include free virus inactivation (1), inhibition of viral uncoating (2), viral genome transcription (3), and viral protein translation and polyprotein processing (4). **d** Photocatalytic process by which TiO2 NPs and TiO2 compounds produce reactive oxygen species to cause disturbance of lipid membranes and damage to genetic information, ultimately resulting in bacterial cell death or viral inactivation (Reproduced with permission from [161], Copyright American Chemical Society 2020)

a small amount (100 ppm) of Ag NPs (Fig. 19) which were found to have significantly improve the antibacterial performance of the treated masks against *Escherichia coli* and *Staphylococcus aureus* bacteria.

Copper and its compounds also have biocidal properties, and their main antimicrobial mechanism is to produce ROS through Cu(I) oxidation. Therefore, these substances have been incorporated into fabrics to provide an antimicrobial function [177, 178]. Borkow et al. [176] impregnated both the exterior and interior layers of N95 face masks with copper oxide (Cu_2O and CuO) (Fig. 19e). These particles provided the face masks with potent anti-influenza biocidal properties without affecting their mechanical filtration performance or causing skin irritation or poisoning through inhalation. The impregnated masks achieved 99.85% filtration of human influenza A (H1N1) and avian influenza (H9N2) viruses, without any viral titres recovering within 30 min. The masks also met the requirements of European EN 14683:2005 and NIOSH N95 standards regarding tests of bacterial filtration efficacy, differential pressure, latex particle challenge, and resistance to penetration by synthetic blood. Additionally, the production cost of these masks was comparable with that of commercial N95 face masks.

The final class of antimicrobial agents in this group is photocatalyst-based NPs. These substances produce ROS to inactivate microbes through light-catalyzed redox reactions [179]. Titanium oxide (TiO_2) and zinc oxide (ZnO) are two common photocatalysts, and TiO_2 NPs have been shown to be able to destroy the lipid membranes of the Newcastle disease virus (NDV) and inhibit its penetration into host cells [180]. Generally, TiO_2 NPs exhibit antimicrobial responses to various critical bacteria and viruses, including *S. aureus*, *E. coli*, *Bacillus subtilis*, *Pseudomonas aeruginosa*, *Staphylococcus aureus*, *Legionella pneumophila*, *Streptococcus*

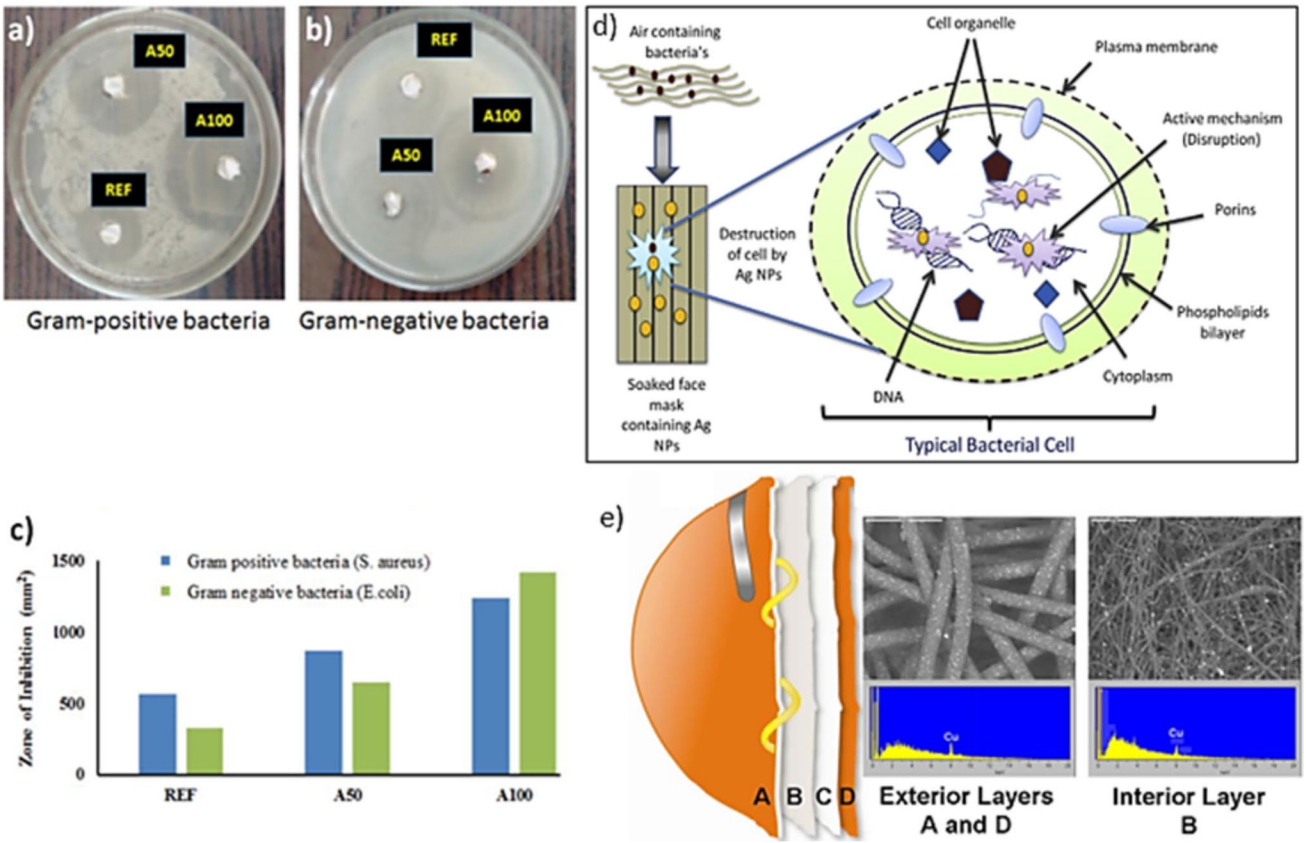

Fig. 19 Antimicrobial face masks using metal-based NPs: Antimicrobial activity with comparison of reference sample (untreated face mask cloth), A50 and A100 with the inhibition zone test for **a** Gram-positive bacteria (*S. aureus*), **b** Gram-negative bacteria (*E. coli*), **c** graph of comparison of zone of inhibition (mm2) of all samples, **d** representative dual antimicrobial mechanism of Ag NPs embedded face mask (Reproduced with permission from [175], Copyright Elsevier, 2018), and **e** anti-influenza copper oxide containing respiratory face mask [176] (Open access)

mutans, vesicular stomatitis virus, and bovine coronavirus [181]. A commercial washable mask with ZnO-coated polyester fabric (inner layer) reduced *E. coli* and *S. aureus* infection by 98% after 1 h of exposure. However, photocatalyst-impregnated masks need to be exposed to sufficient light to attain effective antimicrobial activity, and this is a serious drawback of these antimicrobial agents.

4.1.2 Organic compounds and polymeric coatings

Some natural organic compounds extracted from plants have been shown to have antimicrobial properties. Those of such substances which are less toxic towards humans compared to NPs or other chemical antimicrobial agents have high potential for application in face masks. A commercial antimicrobial face mask containing melt-blown PP filters coated with mangosteen extracts has shown good antibacterial performances against multidrug-resistant tuberculosis, *S. aureus*, and *E. coli* [182], and their non-cytotoxicity and biocompatibility have also been cited. Wang et al. [183] developed antibacterial face masks containing filter cloths made from cotton, polyester fibers, and nonwoven fabric soaked with herbal microcapsules of substances extracted from *Scutellaria baicalensis* (SB) and treated with plasma. These impregnated masks exhibited excellent performance against *E. coli* and *S. aureus* bacteria with antibacterial efficiency above 99%, even after washing 100 times. The bioactive components baicalein and baicalin are responsible for the antibacterial activity of herbal microcapsules. Other antimicrobial organic compounds have been also applied in the fabrication of face masks, such as plant oil extracted from *Plectranthus amboinicus* leaves [184], amino acid–grafted enzymatic hydrolysis lignin [185], and catechin polyphenols [186].

Regarding polymeric antiviral materials, viruses with an intrinsic negative charge are drawn to positive polycations in polymers such as polyethylenimine (PEI) which interfere with their structural or genetic components resulting in full viral disintegration [187, 188]. This type of antiviral coating, which is normally applied by "painting," has been claimed to possess the ability to permanently transmit antiviral and antibacterial qualities even

after being subjected to repeated washing [189]. Another antimicrobial mechanism of polymeric materials is to convey antiviral properties by immobilizing polycations [190, 191]. The titres of viruses have been decreased by immobilized hydrophobic PEI- and dendrimer-based polycations. According to research on the interaction of the bacteriophage PRD1 with PEI-coated glass slides, positive charges and hydrophobicity cause a considerable decline in the viral titre when compared to untreated glass [190]. Generally, the viral titre was decreased even when only polycations were employed (minimum hydrophobicity); however, its combination with acetylated surfaces and positive charges of PEI was more efficient [190]. Coating polyethylene with N-alkylated PEIs also exhibits antiviral effects for non-enveloped viruses [191]. In addition, studies have shown that polyelectrolyte-based techniques can be applied in filtering membranes for antiviral purposes [188]. Several layers of PEI have been produced using a covalent layer-by-layer deposition technique, with terephthalaldehyde serving as the cross-linking agent. In another approach, antiviral characteristics were added to glass and plastic surfaces by coating them with quaternary ammonium compounds (QACs). A thin coating of the QAC polymer was combined with acetone, applied on glass, and allowed to dry to create a positively charged film [192]. This antiviral surface showed a reduction in the viral infectivity of influenza A (H1N1) after 2 min. However, even though QACs are frequently used as antimicrobial materials, their application for medical face masks is severely limited due to toxicity and degradations in performance caused by weak or non-bonded attachment to the filter surface [193, 194], as well as the complexity, ineffectiveness, and unscalability of surface modification using plasma treatment [195] in addition to the low monomeric stability of polymeric antibacterial materials containing pendant QAC [196]. To overcome these limitations, Kumaran et al. [197] reported the development of universal, antiviral, and antibacterial QACs, namely, terpyridine methylammonium chloride (LTMAC) and adenine hexyl ammonium chloride (LAHAC). These can be dip-/spray-coated over conventional mask fabrics to perform the antimicrobial function (Fig. 20a), and method involves the chemical modification of biocompatible lignin molecules with various hydroxyl and carboxyl groups, allowing for a variety of conjugation techniques including the creation of a photopolymerizable coating and functionalization with antimicrobials. Performance testing resulted in large amounts of HCoV-OC43 virus (Fig. 20b) and *Klebsiella pneumoniae* bacteria (Fig. 20c) being eliminated when exposed to spun-bond PP fabric coated with LTMAC and LAHAC.

4.1.3 Graphene

Graphene and its derivatives have been identified as microbial agents [198] owing to their outstanding photothermal and photocatalytic properties [199]. Also, the 2D structure with atomic-scale thickness can itself cause physical damage to bacterial cells [200], and the large surface area of graphene materials provides efficient interaction with the charged residue of virions, hence blocking microorganisms [201]. Therefore, graphene has high potential for application in the fabrication of antimicrobial masks. Zhong et al. [202] assessed the superhydrophobic and photothermal performances of graphene-deposited commercial face masks. The superhydrophobic surfaces were found to prevent droplet penetration through the mask layers, while photothermal generated high temperatures for the masks under solar illumination that can sterilize viruses. Graphene and its derivatives have been also combined with other antimicrobial agents to synergistically enhance antimicrobial efficacy [203]. For example, Zhong et al. [204] proposed the deposition of graphene and silver NPs onto the N95 respirator surface. This combination enhanced photothermal absorption with a plasmonic effect from Ag NPs and superhydrophobic surfaces. In addition, releasing of silver ion also inactivated microbes (Fig. 21).

4.2 Mechanism of antimicrobial filtration functionality

Nanofiber filters are known for their enhanced antimicrobial efficiency compared to conventional filters. With pore diameters typically ranging between 1 and 10 nm, nanofiber filters accomplish the efficient removal of various bacteria, viruses, and organic contaminants [205]. Consequently, while particulate filtration mechanisms can effectively filter ambient microbial aerosols and droplets, recent research has focused on the development of antimicrobial and antiviral filters. Three main strategies have been employed in the fabrication of antimicrobial filters: (i) using polymers which possess antimicrobial properties, (ii) incorporating NPs with antimicrobial effects into the nanofiber matrix, and (iii) coating the filter with bio-antimicrobial molecules. Antimicrobial fibers often rely on the bactericidal effects of integrated agents that disrupt cell membranes in order to achieve their antimicrobial action. The incorporation of these agents helps to combat the growth and presence of harmful microorganisms. Antimicrobial agents operate by disrupting or inhibiting the vital processes of pathogens, including the synthesis of proteins, cell walls, and nucleic acid as well as other metabolic processes (Fig. 22).

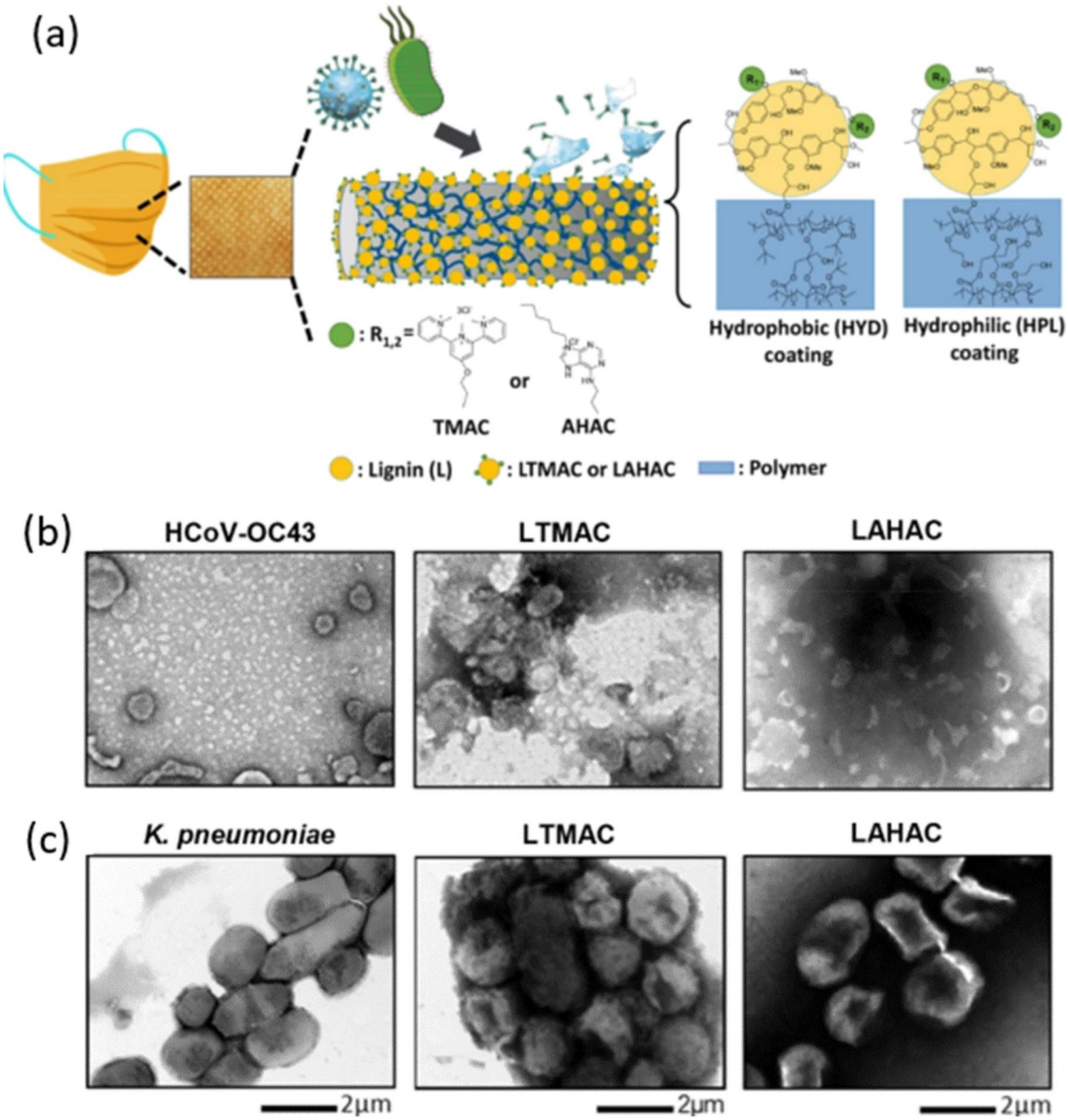

Fig. 20 Antiviral and antibacterial performance of the LTMAC- and LAHAC-coated face mask fabrics: **a** TEM micrographs of the HCoV-OC43 (viral stock as a positive control (left) and virus exposed to spun-bond PP fabrics with HYD LTMAC (middle) and HYD LAHAC (right)) coatings, after 30 min of incubation and TEM micrographs of the *K. pneumoniae* (bacterial stock as a positive control (left) and virus exposed to spun-bond PP fabrics with HYD LTMAC (middle) and HYD LAHAC (right) coatings, after 30 min of incubation) (Reproduced with permission from [197], Copyright 2021 American Chemical Society)

Through various mechanisms, these antimicrobial agents can effectively kill pathogens by neutralizing their ability to grow and cause infections [206]. The antimicrobial agents serve three crucial roles in antimicrobial face masks: (i) boosting antimicrobial effectiveness due to the presence of metal NPs, metallic salts, and quaternary ammonium compounds; (ii) enhancing the self-cleaning attribute through the use of hydrophobic carbon-based nanomaterials such as graphene and CNTs; and (iii) stabilizing the surface electrostatic charges of the antimicrobial filter using triboelectric nanogenerators. Various methods, such as electrospinning, melt blowing, polymerization, chemical grafting, dipping, or spray coating, can be employed to treat filter materials with antimicrobial agents [207].

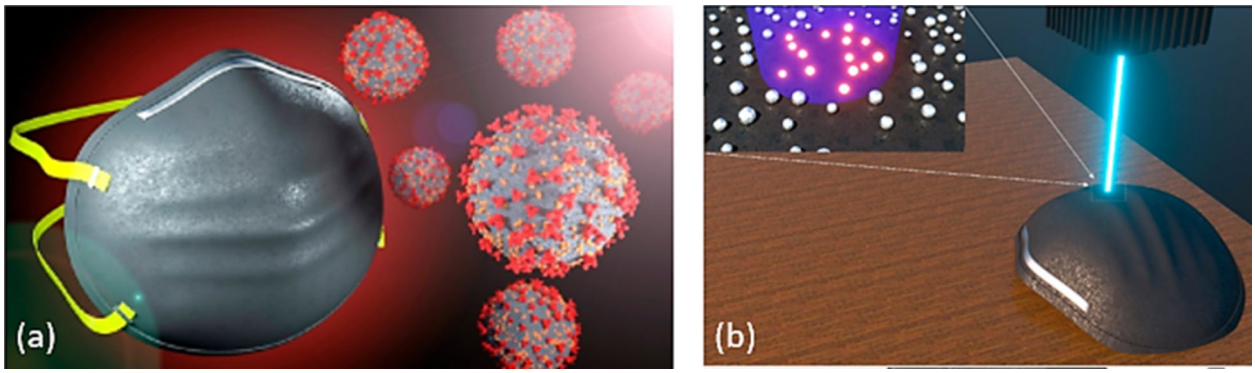

Fig. 21 Plasmonic and superhydrophobic self-decontaminating N95 respirators containing graphene and silver NPs. **b** Illustration of the 405-nm laser diode decontamination. The inset figure illustrates the plasmonic heating of the silver NPs (Reproduced with permission from [204], Copyright 2020 American Chemical Society)

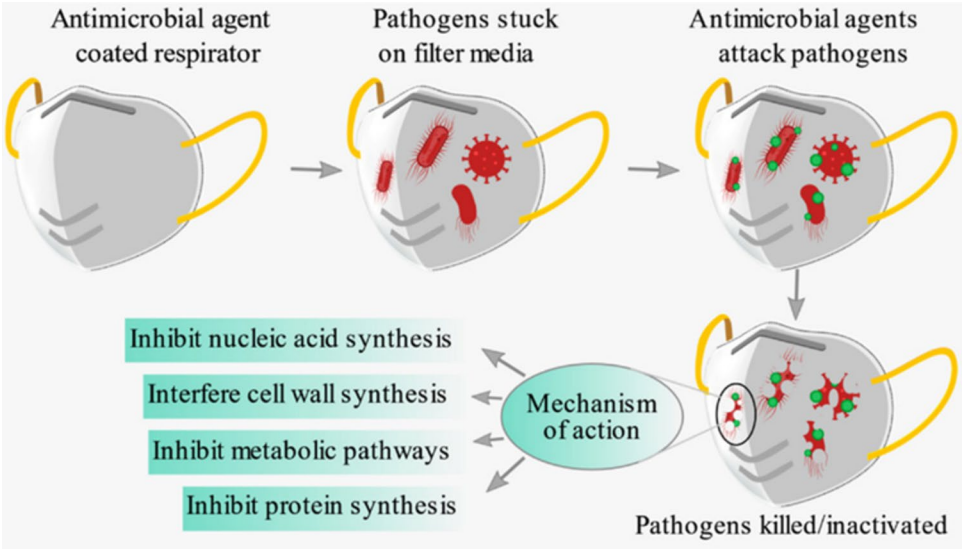

Fig. 22 Schematic drawing for antimicrobial face masks action mechanism to kill or eliminate pathogens [205] (Open access)

4.3 Theoretical work related to antimicrobial filtration functionality

Pathogenic microorganisms such as bacteria and viruses can be transmitted from an infectious source to an individual during breathing, coughing, or sneezing. Several studies have investigated quantitative models for the bacterial filtration efficiency (BFE) and viral filtration efficiency (VFE) of medical face masks. Djeghdir et al. proposed a model to statistically analyze the penetration of small pathogens (100 nm–1 µm) through different types of medical and non-medical face masks [208]. The statistical analysis revealed no significant difference ($p > 0.05$) in BFE and VFE between the masks, while for a slightly larger aerodynamic aerosol size of 2–3 µm, a strong correlation between BFE and VFE was observed with $r = 0.983$. However, the experimental tests showed that the medical masks scored significantly much higher for antimicrobial resistance with values of BFE and VFE of 98% compared to the non-medical filters which had an efficiency of only 65%.

The same research group then investigated the impact of washing parameters, including wash cycles, wash temperature, and use of detergent, on the long-term performance of medical and non-medical face masks [209]. The evaluation of BFE was conducted as follows: an aerosol stream loaded with *S. aureus* Gram-positive bacteria produced through automated nebulizer. The mean particle size (MPS) of bacteria [µm] was 3.0 ± 0.3 µm, and the BFE was calculated as follows:

$$\mathrm{MPS} = \frac{\sum_{i=1}^{6} (\mathrm{Pi} \times \mathrm{Ci})}{\sum_{i=1}^{6} (\mathrm{Ci})} \tag{9}$$

where Pi is 50% of the impactor cutoff diameter (ranging from 0.65 to 7 μm) and Ci is the number of colony-forming units (CFUs) grown at the i-th stage of positive runs (without a mask). By applying this formula over six runs, the BFE is then calculated as

$$BFC = \frac{C - T}{C \times 100} \tag{10}$$

where C is the mean of the positive CFUs runs and T is the total CFUs of the six stages count plates.

Although the value of BFE for medical face masks was higher than that for non-medical masks, the resistance of the latter to washing was much better with almost no change in BFE after washing with detergent.

4.4 Efficiency of antimicrobial filtration functionality

The reusability and long-term antimicrobial filtration efficiency of nanofiber face masks have recently been enhanced due to the use of three innovative technologies [32, 210–213]. The first approach involves the functionalization of nonwoven fabrics by coating with salt (NaCl, KCl, K_2SO_4,) [205], which capitalizes on the unique property of salt to dissolve upon contact with viruses and then recrystallize upon drying. The resulting antipathogenic activity based on recrystallization capability has been successfully demonstrated using sodium chloride (NaCl) to treat filter membranes, resulting in highly effective antimicrobial filtration systems [214, 215]. An innovative salt-coated nanofibrous membrane was first introduced for pathogen filtration under harsh environmental conditions [213]. The salt-functionalized membranes demonstrated a substantial increase in filtration efficiency compared to bare membranes, with differences of up to 48%. Remarkably, even the thickest salt filters tested maintained high breathability, surpassing commercial surgical masks by over 60%. In addition to enhanced filtration, the salt-functionalized filters exhibited the rapid inactivation of both Gram-positive and Gram-negative bacteria, with CFU reductions observed within just 5 min. Furthermore, in vivo testing revealed structural damage to bacteria due to salt recrystallization, confirming the efficiency of salt-functionalized filters in real-world conditions. A noteworthy aspect of salt-functionalized membranes is the resilience of the salt coatings under harsh environmental conditions, including at 37 °C and varying relative humidity levels of 70–90%. This indicates the robust nature of the pathogen inactivation capability, ensuring consistent performance even in challenging scenarios.

The second technique is based on coating the nanofiber with photoactive/photocatalytic materials, such as metal NPs, graphene, or carbon materials, which imparts photothermal and photocatalytic activity to the masks [32, 216–218]. This technology utilizes solar radiation to elevate temperature and dissipate heat, effectively killing pathogens [219, 220]. Furthermore, the antibacterial coating serves a dual purpose by preventing bacterial colonization on the surfaces of the material and functioning as a barrier to permeation. Several studies have reported the efficiency of zinc oxide (ZnO) as a photocatalyst material for bacterial inactivation [221]. The creation of self-cleaning nanofiber involving the functionalization of silicone-based (polydimethylsiloxane, PDMS) fibrous membranes with a photocatalyst was recently reported [222]. The PDMS nanofiber was coated with ZnO NPs using either colloid-electrospinning or post-functionalization procedures. Nanofiber enhanced with ZnO NPs exhibits the ability to degrade a photosensitive dye and demonstrates antibacterial properties against both Gram-positive and Gram-negative bacteria. This antimicrobial effect was attributed to the generation of reactive oxygen species upon exposure to UV light. Additionally, the functionalized PDMS/ZnO membrane exhibited 65% filtration efficiency against PM1.0.

The third technique focuses on embedding metal NPs and metal–organic frameworks (MOFs) in the filter matrix. A recent study has shown that incorporating zinc ions into polyamide fabrics and utilizing copper/zeolitic imidazolate framework Cu/ZIF-8 core–shell nanowire filters enhance the effectiveness of reusable face masks. These innovations demonstrate the ability to deactivate both bacteria and viruses, contributing to the development of more efficient and sustainable protective face masks. A few other studies have explored silicon- and polyamide-based filter materials for respiratory applications. For example, an Si-based, replaceable, flexible, and nanoporous polymeric membrane was manufactured by electrospinning [223], and the polymeric membrane not only effectively filters microorganisms but also possesses self-cleaning properties, enhancing its longevity and usability. A novel, highly efficient, renewable, and antibacterial N-halamine nanofibrous membrane for respirators based on polyamide has also been developed using an approach which involved a one-step facile chlorination process [224]. The resulting filter can be easily renewed and reused, contributing to the sustainability of respiratory protection measures. These technological advances signal the potential for

the development of reusable antimicrobial masks using diverse mechanisms, ensuring both pathogen inactivation and environmental responsibility.

5 Future work

5.1 Synergistic combination of mechanical and electrostatic filtration and antimicrobial functionality

Researchers are actively exploring the integration of mechanical and electrostatic filtration principles along with antimicrobial functionality to leverage the strengths of each method. The goal is to design multifunctional nanofiber structures capable of efficiently capturing particles through both physical and electrostatic mechanisms in addition to their potential for the inactivation of pathogens [95, 225–229]. This innovative approach aims to enhance overall filtration efficiency and to broaden the range of particle sizes that face masks can effectively capture, where the combination of these principles may allow the development of more effective and versatile filtration systems. In one study, aligned PLA electrospun nanofiber membranes have been fabricated to investigate the effect of degree of alignment on both mechanical and electrostatic filtration [95]. It was found that increasing the alignment degree up to a certain threshold resulted in smaller pore sizes within the nanofiber. This contrasted with randomly aligned nanofiber which had larger pores and lower filtration efficiency. Additionally, changes in the geometry of the PLA nanofiber were found to influence the surface potential of the membrane. Aligned nanofiber exhibited a maximum surface potential of 71 V, contributing to high electrostatic removal efficiency. These findings suggest that the alignment of nanofiber significantly impacts both the mechanical and electrostatic properties of the membrane, ultimately leading to enhanced efficiency in removing particles through the combination of mechanical and electrostatic filtration mechanisms. The emerging concepts of "smart" and "multifunctional" face masks are gaining traction given advances in current face mask technologies. Such masks are designed to incorporate features of superhydrophobicity, reusability, and antiviral/antibacterial ability. Accordingly, several research studies have introduced multifunctional face masks which represent hybrid mechanical, electrostatic, and antimicrobial filtration processes. An electropolarized poly(vinylidene fluoride-trifluoroethylene) (PVDF-TrFE) nanofiber membrane decorated with Li-doped ZnO nanorods has been manufactured to enhance the filtering capability and antibacterial activity of an ultrathin air filter [226]. The filter was electropolarized to increase its coulombic interaction with PM and *S. aureus*, and an impressive removal efficiency of up to 90% for PM1.0 was demonstrated along with a remarkable sterilization rate of 99.5% against *S. aureus*. Mechanical and antimicrobial filtration have been also been achieved using multifunctional free-standing nanoarchitecture networks with an average diameter of 20 nm [229]. The ULTRA NET filters had an optimal pore structure and exceptionally low thickness of approximately 350 nm and achieved a high removal efficiency of 99.98% with a very low pressure drop of 0.07% for PM0.3. Furthermore, the extremely small pores of this filter exhibited mechanical sieving protection against *S. aureus* with an inactivation efficiency of > 99.5%. Meanwhile, a TENG functional and eco-friendly polymeric nanofiber face mask composed of a polybutylene adipate terephthalate (PBAT) matrix blended with cetyltrimethylammonium bromide (CTAB) and montmorillonite (MMT) clay exhibited outstanding filtration performance, reaching 98.3% for PM0.3 with a noticeably low pressure drop of 40 Pa [230]. Additionally, it achieved levels of antibacterial performance of 99.8% against *S. aureus*, 99.79% against influenza, and 99.99% against human coronavirus.

5.2 Breakthroughs in antimicrobial functionality

The development of surfaces with antiviral properties is essential to minimize the risk of the transmission of disease through surface contact. While some viruses become inactive quickly on surfaces, others can remain viable for extended periods, thus posing a significant transmission risk. There is a pressing need for cost-effective and sustainable technological solutions to prevent virus activation on face mask surfaces and to contribute to overall risk control [210].

Various methods have been utilized to create antiviral face masks based on doping with antiviral agents or coating with functional materials. For example, Wang et al. engineered a biocatalytic composite of polydopamine (PDA) matrix coated with perhydrolase (AcT) [231]. When applied to different surfaces, this AcT–PDA coating significantly reduced the infectivity of a SARS-CoV-2 pseudo-virus within minutes. Another approach involved a polyester nanofiber coating with a poly(dimethyl amino methyl) styrene-co-1H,1H,2H,2H-perfluorodecyl acrylate (PDP), which exhibited strong antiviral activity and biocompatibility [146]. The positive surface potential of the PDP-coated fabric facilitated electrostatic interaction with negatively charged bacteria and viruses, leading to microbial inactivation. Moreover, the oleophobic nature and hydrophobicity of the PDP layer prevented the attachment of moisture and contaminants to the membrane surface.

A water-borne spray coating comprised of polystyrene and macroCTA nanoworms has demonstrated a noteworthy capacity to deactivate influenza and SARS-CoV-2

by breaking down viral RNA within 30 min [220]. This nanoscale coating performed conformational alterations upon binding to viral droplets leading to rupturing of the viral membrane. Moreover, the incorporation of a covalently attached fluorescent polygalactose to the nanoworm surface was functionalized as a novel approach for the reapplication of the coated layer in order to sustain a consistently high level of antiviral effectiveness on the fabric surface.

NPs, including silver, copper, and various antimicrobial agents, are being integrated into nanofiber matrices to develop surfaces that actively neutralize pathogens [232]. Furthermore, there is an ongoing exploration of responsive materials which are capable of delivering the controlled release of antimicrobial agents, thereby ensuring prolonged and efficient protection [31, 233]. Silver nanowires electrospray coated onto polyacrylonitrile (PAN) nanofiber membrane have demonstrated outstanding antiviral deactivation against bacteriophage MS2 [234]. Similarly, Chen et al. explored the potential of graphene oxide/silver (GO/Ag) nanocomposites to kill feline coronavirus (FCoV), which is a positive-stranded RNA virus that could infect cats worldwide [235]. The authors concluded that the higher percentage inhibition of FCoV was achieved at higher concentrations of GO and GO/Ag. This implies that Ag-based nanocoating, including Ag nanowires and GO/Ag nanocomposites, has the potential to enhance antiviral efficiency on various surfaces, including those of face masks.

Author contribution BL and NO: writing—original draft; EE: review and editing; and AHH, KM, NS, and IS: supervision and data correction. All authors have read and agreed to the published version of the manuscript.

Funding This paper is based upon work supported by Science, Technology & Innovation Funding Authority (STDF) under grant number 43944 and the British Council (Impact Scheme) of grant number 624494545.

Data Availability Data will be available based on any request as we will send it by email to the requestor.

Declarations

Ethical approval Not applicable.

Competing interests The authors declare no competing interests.

References

1. P.J. Landrigan, Air pollution and health. The Lancet Public Health **2**(1), e4–e5 (2017)
2. R.D. Brook et al., Particulate matter air pollution and cardiovascular disease: An update to the scientific statement from the American Heart Association. Circulation **121**(21), 2331–2378 (2010)
3. V. Després, J.A. Huffman, S.M. Burrows, C. Hoose, A. Safatov, G. Buryak, J. Fröhlich-Nowoisky, W. Elbert, M. Andreae, U. Pöschl, R. Jaenicke, Primary biological aerosol particles in the atmosphere: A review. Tellus B: Chemical and Physical Meteorology **64**(1), 15598 (2012)
4. L. Setti, SARS-Cov-2RNA found on particulate matter of Bergamo in Northern Italy: First evidence. Environ. Res. **188**(2020)
5. Wu, X., Nethery, R. C., Sabath, M. B., Braun, D., & Dominici, F, Exposure to air pollution and COVID-19 mortality in the United States: A nationwide cross-sectional study. MedRxiv, 20054502. (2020)
6. A.G. Harrison, T. Lin, P. Wang, Mechanisms of SARS-CoV-2 transmission and pathogenesis. Trends Immunol. **41**(12), 1100–1115 (2020)
7. Hinds, W.C. and Y. Zhu, Aerosol Technology: Properties, behavior, and measurement of airborne particles. 2022: John Wiley & Sons.
8. Elnabawy, E., Sun, D., Shearer, N. Shyha, I, New insight into the effect of electric field and airflow hybridized forces on the production yield and characteristics of nanofiber membranes. Journal of Science: Advanced Materials and Devices, 100552 (2023)
9. Scaffaro, R., and M.C. Citarrella, Nanofibrous polymeric membranes for air filtration application: A review of progress after the COVID-19 pandemic. Macromolecular Materials and Engineering, 2300072 (2023)
10. Y. Zhou, Y. Liu, M. Zhang, Z. Feng, D.G. Yu, K. Wang, Electrospun nanofiber membranes for air filtration: A review. Nanomaterials **12**(7), 1077 (2022)
11. S. Han, J. Kim, S.H. Ko, Advances in air filtration technologies: Structure-based and interaction-based approaches. Materials Today Advances **9**, 100134 (2021)
12. A. Kakoria, S. Sinha-Ray, Ultrafine nanofiber-based high efficiency air filter from waste cigarette butts. Polymer **255**, 125121 (2022)
13. Al-Attabi, R., She, F., Zhao, S., Dumée, L.F., Schütz, J.A., Xing, W., Zhong, Z. & Kong, L., Durable and comfortable electrospun nanofiber membranes for face mask applications. Separation and Purification Technology. 124370 (2023)
14. Y. Wu, X. Li, Q. Zhong, F. Wang, B. Yang, (2023), *Preparation and filtration performance of antibacterial PVDF/SiO2/Ag composite nanofiber membrane*. Journal of Building Engineering **74**, 106864 (2023)
15. L. Zhang, Q. Zheng, X. Ge, H. Chan, G. Zhang, K. Fang, Y. Liang, (2023), *Preparation of nylon-6 micro-nanofiber composite membranes with 3D uniform gradient structure for high-efficiency air filtration of ultrafine particles*. Sep. Purif. Technol. **308**, 122921 (2023)
16. A.I. Kamil, M.M. Munir, Structure and morphology optimization of nanofiber membrane for the application of

high-performance air filtration. Powder Technol. **430**, 118978 (2023)
17. B. Yang, M. Hao, Z. Huang, Z. Chen, Y. Liu, High filterable electrospun nanofibrous membrane with charged electret after electrification treatment for air filtration. Fibers and Polymers **24**(3), 921–929 (2023)
18. Yang, Y., Yang, Y., Huang, J., Li, S., Meng, Z., Cai, W., & Lai, Y., Electrospun nanocomposite fibrous membranes for sustainable face mask based on triboelectric nanogenerator with high air filtration efficiency. Advanced Fiber Materials, 1–14 (2023)
19. S. Zhang, N. Wang, Q. Zhang, R. Guan, Z. Qu, L. Sun, J. Li, The rise of electroactive materials in face masks for preventing virus infections. ACS Applied Materials & Interfaces **15**(42), 48839–48854 (2023)
20. Liu, C., Hsu, P. C., Lee, H. W., Ye, M., Zheng, G., Liu, N., ... & Cui, Y., *Transparent air filter for high-efficiency PM2. 5 capture.* Nature communications. **6**(1): 6205 (2015)
21. Vázquez-López, A., Ao, X., del Río Saez, J. S., & Wang, D. Y. , *Triboelectric nanogenerator (TENG) enhanced air filtering and face masks: Recent advances.* Nano Energy,108635 (2023)
22. M. Nifuku, Y. Zhou, A. Kisiel, T. Kobayashi, H. Katoh, Charging characteristics for electret filter materials. J. Electrostat. **51**, 200–205 (2001)
23. H. Zhang, J. Liu, X. Zhang, C. Huang, X. Jin, Design of electret polypropylene melt blown air filtration material containing nucleating agent for effective PM2. 5 capture. RSC advances. **8**(15), 7932–7941 (2018)
24. H. Liu, S. Zhang, L. Liu, J. Yu, B. Ding, High-performance PM0. 3 air filters using self-polarized electret nanofiber/nets. Advanced Functional Materials **30**(13), 1909554 (2020)
25. D.Y. Choi, S.H. Jung, D.K. Song, E.J. An, D. Park, T.O. Kim, J.H. Jung, H.M. Lee, Al-coated conductive fibrous filter with low pressure drop for efficient electrostatic capture of ultrafine particulate pollutants. ACS applied materials & interfaces **9**(19), 16495–16504 (2017)
26. G. Pullangott, U. Kannan, S. Gayathri, D.V. Kiran, S.M. Maliyekkal, A comprehensive review on antimicrobial face masks: An emerging weapon in fighting pandemics. RSC Adv. **11**(12), 6544–6576 (2012)
27. S.S. Athukoralalage, C.A. Bell, A.C. Gemmell, A.E. Rowan, N. Amiralian, Recent advances and future perspectives in engineering biodegradable face masks. Journal of Materials Chemistry A **11**, 1575–1592 (2023)
28. A.D. Iuliano, K.M. Roguski, H.H. Chang, D.J. Muscatello, R. Palekar, S. Tempia, C. Cohen, J.M. Gran, D. Schanzer, B.J. Cowling, P. Wu, Estimates of global seasonal influenza-associated respiratory mortality: A modelling study. The Lancet **391**(10127), 1285–1300 (2018)
29. https://www.who.int/news/item/13-12-2017-up-to-650-000-people-die-of-respiratory-diseases-linked-to-seasonal-flu-each-year.
30. I.H. Ali, A.M. Elkashlan, M.A. Hammad, M. Hamdi, Antimicrobial and anti-SARS-CoV-2 activities of smart daclatasvir-chitosan/gelatin nanoparticles-in-PLLA nanofibers medical textiles; in vitro, and in vivo study. International Journal of Biological Macromolecules **253**, 127350 (2023)
31. Song, Y., Lee, Y.K., Lee, Y., Hwang, W.T., Lee, J., Park, S., Park, N., Song, H., Kim, H., Lee, K.G. & Kim, I.D., Anti-viral, antibacterial, but non-cytotoxic nanocoating for reusable face mask with efficient filtration, breathability, and robustness in humid environment. Chem. Eng. Js. 144224 (2023)
32. K. Geetha, D. Sivasangari, H.S. Kim, G. Murugadoss, A. Kathalingam, Electrospun nanofibrous ZnO/PVA/PVP composite films for efficient antimicrobial face masks. Ceram. Int. **48**(19), 29197–29204 (2022)
33. R. He, J. Li, M. Chen, S. Zhang, Y. Cheng, X. Ning, N. Wang, Tailoring moisture electroactive Ag/Zn@ cotton coupled with electrospun PVDF/PS nanofibers for antimicrobial face masks. J. Hazard. Mater. **428**, 128239 (2022)
34. A. Cimini, E. Imperi, A. Picano, M. Rossi, Electrospun nanofibers for medical face mask with protection capabilities against viruses: State of the art and perspective for industrial scale-up. Appl. Mater. Today **32**, 101833 (2023)
35. Akduman, C. & E.A. Kumbasar. Nanofibers in face masks and respirators to provide better protection. in IOP conference series: Materials science and engineering. Vol. 460, p. 012013. IOP Publishing, (2018)
36. F.N. Karabulut et al., Electrospun nanofibre filtration media to protect against biological or nonbiological airborne particles. Polymers **13**(19), 3257 (2021)
37. I. Kulmala, K. Heinonen, S. Salo, Improving filtration efficacy of medical face masks. Aerosol. Air Qual. Res. **21**(6), 210043 (2021)
38. S.D. Skaria, G.C. Smaldone, Respiratory source control using surgical masks with nanofiber media. Ann. Occup. Hyg. **58**(6), 771–781 (2014)
39. Y. Bian et al., Influence of fiber diameter, filter thickness, and packing density on PM2. 5 removal efficiency of electrospun nanofiber air filters for indoor applications. Build. Environ. **170**, 106628 (2020)
40. D.P. Bonfim et al., Development of filter media by electrospinning for air filtration of nanoparticles from PET bottles. Membranes **11**(4), 293 (2021)
41. L. Wei, H. Zhang, X. Qin, Fabricated narrow diameter distribution nanofiber for an air filtration membrane using a double rings slit spinneret. Text. Res. J. **89**(6), 936–947 (2019)
42. H.B. Kim et al., Filter quality factors of fibrous filters with different fiber diameter. Aerosol Sci. Technol. **55**(2), 154–166 (2021)
43. A. Podgórski, A. Bałazy, L. Gradoń, Application of nanofibers to improve the filtration efficiency of the most penetrating aerosol particles in fibrous filters. Chem. Eng. Sci. **61**(20), 6804–6815 (2006)
44. Li, X., & Gong, Y., Design of polymeric nanofiber gauze mask to prevent inhaling PM2. 5 particles from haze pollution. J. Chem. 460392 (2015)
45. L. Wang et al., Biodegradable and high-performance multiscale structured nanofiber membrane as mask filter media via poly (lactic acid) electrospinning. J. Colloid Interface Sci. **606**, 961–970 (2022)
46. C. Wang et al., Silk nanofibers as high efficient and lightweight air filter. Nano. Res. **9**(9), 2590–2597 (2016)
47. R. Chen et al., Thermoplastic polyurethane nanofiber membrane based air filters for efficient removal of ultrafine particulate matter PM0 1. ACS Appl. Nano Mater. **4**(1), 182–189 (2020)
48. W.W.-F. Leung, C.-H. Hung, P.-T. Yuen, Effect of face velocity, nanofiber packing density and thickness on filtration performance of filters with nanofibers coated on a substrate. Sep. Purif. Technol. **71**(1), 30–37 (2010)
49. L. Zhong et al., Ultra-fine SiO2 nanofilament-based PMIA: A double network membrane for efficient filtration of PM particles. Sep. Purif. Technol. **202**, 357–364 (2018)
50. J. Li et al., Nest-like multilevel structured graphene oxide-on-polyacrylonitrile membranes for highly efficient filtration of ultrafine particles. J. Materiomics **5**(3), 422–427 (2019)
51. S. Zhang et al., A controlled design of ripple-like polyamide-6 nanofiber/nets membrane for high-efficiency air filter. Small **13**(10), 1603151 (2017)
52. H. Liu et al., High-efficiency and super-breathable air filters based on biomimetic ultrathin nanofiber networks. Compos. Commun. **22**, 100493 (2020)
53. H. Liu et al., A fluffy dual-network structured nanofiber/net filter enables high-efficiency air filtration. Adv. Func. Mater. **29**(39), 1904108 (2019)

54. O. Yildiz, P.D. Bradford, Aligned carbon nanotube sheet high efficiency particulate air filters. Carbon **64**, 295–304 (2013)
55. K.M. Yun et al., Nanoparticle filtration by electrospun polymer fibers. Chem. Eng. Sci. **62**(17), 4751–4759 (2007)
56. K.-S. Lee et al., Filter layer structure effect on the most penetrating particle size of multilayered flat sheet filter. Powder Technol. **344**, 270–277 (2019)
57. Y. Chuanfang, Aerosol filtration application using fibrous media—An industrial perspective. Chin. J. Chem. Eng. **20**(1), 1–9 (2012)
58. L. Janssen, Principles of physiology and respirator performance. Occup. Health Saf. **72**(6), 73–81 (2003)
59. W. Hao et al., Filtration performances of non-medical materials as candidates for manufacturing facemasks and respirators. Int. J. Hyg. Environ. Health **229**, 113582 (2020)
60. M.D. Durham, D.A. Lundgren, Evaluation of aerosol aspiration efficiency as a function of Stokes number, velocity ratio and nozzle angle. J. Aerosol Sci. **11**(2), 179–188 (1980)
61. C.Y. Chen, Filtration of aerosols by fibrous media. Chem. Rev. **55**(3), 595–623 (1955)
62. W.W.F. Leung, Q. Sun, Electrostatic charged nanofiber filter for filtering airborne novel coronavirus (COVID-19) and nanoaerosols. Sep. Purif. Technol. **250**, 116886 (2020)
63. A. Konda et al., Aerosol filtration efficiency of common fabrics used in respiratory cloth masks. ACS Nano **14**(5), 6339–6347 (2020)
64. A. Tcharkhtchi et al., An overview of filtration efficiency through the masks: Mechanisms of the aerosols penetration. Bioactive materials **6**(1), 106–122 (2021)
65. L. Maduna, A. Patnaik, Textiles in air filtration. Text. Prog. **49**(4), 173–247 (2017)
66. Mörters, P., & Peres, Y., Brownian motion, Vol. 30, Cambridge University Press, (2010)
67. A. Sanyal, & Sinha-Ray, S, *Ultrafine PVDF nanofibers for filtration of air-borne particulate matters: A comprehensive review*. Polymers **13**(11), 1864 (2021)
68. Stafford, R. G., & Ettinger, H. J., *Filter efficiency vs particle size and velocity* (No. LA-4650). Los Alamos National Lab.(LANL), Los Alamos, NM (United States), (1971)
69. Y. Qian et al., Performance of N95 respirators: Filtration efficiency for airborne microbial and inert particles. Am. Ind. Hyg. Assoc. J. **59**(2), 128–132 (1998)
70. C.H. Hung, W.W. Leung, F, *Filtration of nano-aerosol using nanofiber filter under low Peclet number and transitional flow regime*. Sep. Purif. Technol. **79**(1), 34–42 (2011)
71. S.-H. Huang et al., Factors affecting filter penetration and quality factor of particulate respirators. Aerosol and Air Quality Research **13**(1), 162–171 (2013)
72. W.C. HindS, *Filtration, aerosol technology* (John Wiley and Sons Inc., New York, 1982)
73. R.C. Brown, *Air filtration: An integrated approach to the theory and applications of fibrous filters* (Pergamon Press, Oxford, 1993)
74. I. Stechkina, A. Kirsch, N. Fuchs, Studies on fibrous aerosol filters—iv calculation of aerosol deposition in model filters in the range of maximum penetration. Ann. Occup. Hyg. **12**(1), 1–8 (1969)
75. J. Pich, *Gas filtration theory, filtration-principles and practices, M* (Dekker, New York, 1977)
76. Z. Zhang, B.Y. Liu, Experimental study of aerosol filtration in the transition flow regime. Aerosol Sci. Technol. **16**(4), 227–235 (1992)
77. S. Jennings, The mean free path in air. J. Aerosol Sci. **19**(2), 159–166 (1988)
78. S. Kuwabara, The forces experienced by randomly distributed parallel circular cylinders or spheres in a viscous flow at small Reynolds numbers. J. Phys. Soc. Jpn. **14**(4), 527–532 (1959)
79. A. Sanyal, S. Sinha-Ray, Ultrafine PVDF nanofibers for filtration of air-borne particulate matters: A comprehensive review. Polymers **13**(11), 1864 (2021)
80. S. Yan et al., The formation of ultrafine polyamide 6 nanofiber membranes with needleless electrospinning for air filtration. Polym. Adv. Technol. **30**(7), 1635–1643 (2019)
81. P. Li et al., Air filtration in the free molecular flow regime: A review of high-efficiency particulate air filters based on carbon nanotubes. Small **10**(22), 4543–4561 (2014)
82. Z. Wang, C. Zhao, Z. Pan, Porous bead-on-string poly (lactic acid) fibrous membranes for air filtration. J. Colloid Interface Sci. **441**, 121–129 (2015)
83. J.J. Huang et al., Fabrication of bead-on-string polyacrylonitrile nanofibrous air filters with superior filtration efficiency and ultralow pressure drop. Sep. Purif. Technol. **237**, 116377 (2020)
84. V. Kadam et al., Electrospun bilayer nanomembrane with hierarchical placement of bead-on-string and fibers for low resistance respiratory air filtration. Sep. Purif. Technol. **224**, 247–254 (2019)
85. R. Mostofi, B. Wang, F. Haghighat, A. Bahloul, L. Jaime, Performance of mechanical filters and respirators for capturing nanoparticles-Limitations and future direction. Ind. Health **48**(3), 296–304 (2010)
86. G. Liu, M. Xiao, X. Zhang, C. Gal, X. Chen, L. Liu, S. Pan, J. Wu, L. Tang, D. Clements-Croome, A review of air filtration technologies for sustainable and healthy building ventilation. Sustainable cities and society **32**, 375–396 (2017)
87. Derk, R.C., Coyle, J.P., Lindsley, W.G., Blachere, F.M., Lemons, A.R., Service, S.K., Martin Jr, S.B., Mead, K.R., Fotta, S.A., Reynolds, J.S. & McKinney, W.G., Efficacy of do-it-yourself air filtration units in reducing exposure to simulated respiratory aerosols. Building and environment. **229**, 109920 (2023)
88. H. Kabrein, M.Z.M. Yusof, A.M. Leman, (2016), Progresses of filtration for removing particles and gases pollutants of indoor; limitations and future direction; review article. ARPN J Eng Appl Sci **11**, 3633–3639 (2016)
89. M.K. Kisomi, S. Seddighi, R. Mohammadpour, A. Rezaniakolaei, Enhancing air filtration efficiency with triboelectric nanogenerators in face masks and industrial filters. Nano Energy **2023**(112), 108514 (2023)
90. C.L. Li, W.Z. Song, D.J. Sun, M. Zhang, J. Zhang, Y.Q. Chen, S. Ramakrishna, Y.Z. Long, A self-priming air filtration system based on triboelectric nanogenerator for active air purification. Chemical Engineering Journal **452** 139428 (2023)
91. F.D.A. Lima, G.B. Medeiros, P.A.M. Chagas, M.L. Aguiar, V.G. Guerra, (2023), Aerosol nanoparticle control by electrostatic precipitation and filtration processes—A review. Powders **2**(2), 259–298 (2023)
92. G.C. da Mata, M.S. Morais, W.P. de Oliveira, M.L. Aguiar, Sustainable surgical masks: Optimizing fine/ultrafine particle filtration using PVA/chitosan electrospun nanofibers. Environ. Sci. Nano **10**(8), 2185–2200 (2023)
93. Y. Wang, X. Zhang, X. Jin, W. Liu, An in situ self-charging triboelectric air filter with high removal efficiency, ultra-low pressure drop, superior filtration stability, and robust service life. Nano Energy **105**, 108021 (2023)
94. A. Lakshmanan, G. Marappan, D. Sarkar, Electric field activated ON/OFF surface charge polarization of transparent filter media for high-efficiency PM2. 5 filtration. Chem. Eng. J. **461**, 142023 (2023)
95. M. Kashif, H. Guo, J. Ge, X. Lv, S. Rasul, Y. Liu, Effect of different symmetries of electrospun poly (lactic acid) nanofibers

on facemask filtration. ACS Applied Polymer Materials **5**(8), 5995–6002 (2023)
96. Z. Wang, Z. Zhang, Z. Peng, X. Yang, X. Li, Y. Shan, B. Liu, X. Xu, Z. Yang, Self-charging and long-term face masks leveraging low-cost, biodegradable and sustainable piezoelectric nanofiber membrane. (2023)
97. S. Wanwong, W. Sangkhun, P. Jiamboonsri, Electrospun cyclodextrin/poly (L-lactic acid) nanofibers for efficient air filter: Their PM and VOC removal efficiency and triboelectric outputs. Polymers **15**(3), 722 (2023)
98. Y. Gao, E. Tian, Y. Zhang, J. Mo, Utilizing electrostatic effect in fibrous filters for efficient airborne particles removal: Principles, fabrication, and material properties. Appl. Mater. Today **2022**(26), 101369 (2022)
99. Tian, E., Gao, Y., & Mo, J., Experimental studies on electrostatic-force strengthened particulate matter filtration for built environments: Progress and perspectives. Building and Environment. 228,109782. (2022)
100. M. Bandi, Electrocharged facepiece respirator fabrics using common materials. Proc. Royal Soc. A **476**(2243), 20200469 (2020)
101. M. Bandi, N95-electrocharged filtration principle based face mask design using common materials. Okinawa Institute of Science and Technology Graduate University, (2020)
102. R. Lathrache, H. Fissan, Enhancement of particle deposition in filters due to electrostatic effects. Filtr. Sep. **24**(6), 418–422 (1987)
103. E. Tian, Y. Gao, J. Mo, Experimental studies on electrostatic-force strengthened particulate matter filtration for built environments Progress and perspectives. Build. Environ. **228**, 109782 (2023)
104. S. Yang, W.G. Lee, *Electrostatic enhancement of collection efficiency of the fibrous filter pretreated with ionic surfactants*. J. Air Waste Manag. Assoc. **55**(5), 594–603 (2005)
105. Bergman, W., A. Biermann, and W. Kuhl, *Electric air filtration: Theory, laboratory studies, hardware development, and field evaluations*. 1983, Lawrence Livermore National Lab.
106. R.M. Eninger, T. Honda, A. Adhikari, H. Heinonen-Tanski, T. Reponen, S.A. Grinshpun, Filter performance of N99 and N95 facepiece respirators against viruses and ultrafine particles. Ann. Occup. Hyg. **52**(5), 385–396 (2008)
107. R. Givehchi, Q. Li, Z. Tan, The effect of electrostatic forces on filtration efficiency of granular filters. Powder Technol. **277**, 135–140 (2015)
108. D.Y. Choi et al., Al-coated conductive fibrous filter with low pressure drop for efficient electrostatic capture of ultrafine particulate pollutants. ACS Appl. Mater. Interfaces. **9**(19), 16495–16504 (2017)
109. K.M. Sim et al., Antimicrobial nanoparticle-coated electrostatic air filter with high filtration efficiency and low pressure drop. Sci. Total Environ. **533**, 266–274 (2015)
110. Q. Ou et al., Evaluation of decontamination methods for commercial and alternative respirator and mask materials–view from filtration aspect. J. Aerosol Sci. **150**, 105609 (2020)
111. R.R. Cai, L.Z. Zhang, A.B. Bao, PM collection performance of electret filters electrospun with different dielectric materials-a numerical modeling and experimental study. Build. Environ. **131**, 210–219 (2018)
112. S.H. Yousefi, H.V. Tafreshi, Modeling electrospun fibrous structures with embedded spacer particles: Application to aerosol filtration. Sep. Purif. Technol. **235**, 116184 (2020)
113. J. He, J. Liu, L. Kong, P. Wang, X. Zhang, Simulation study of a novel cylindrical micro-electrostatic particulate air filter with high filtration efficiency and low resistance. Buildings **11**(10), 465 (2021)
114. L. Hou, A. Zhou, X. He et al., CFD simulation of the filtration performance of fibrous filter considering fiber electric potential field. Trans. Tianjin Univ **25**, 437–450 (2019)
115. J. Kim, W.J. Jasper, J.P. Hinestroza, Charge characterization of an electrically charged fiber via electrostatic force microscopy. J. Eng. Fibers Fabr. **1**(2), 155892500600100200 (2006)
116. J. Xu et al., Roll-to-roll transfer of electrospun nanofiber film for high-efficiency transparent air filter. Nano Lett. **16**(2), 1270–1275 (2016)
117. R. Thakur, D. Das, A. Das, Electret air filters. Sep. Purif. Rev. **42**(2), 87–129 (2013)
118. P.P. Tsai, H. Schreuder-Gibson, P. Gibson, Different electrostatic methods for making electret filters. J. Electrostat. **54**(3–4), 333–341 (2002)
119. Le, T.T., et al., *Piezoelectric nanofiber membrane for reusable, stable, and highly functional face mask filter with long-term biodegradability.* Advanced Functional Materials 2113040 (2022)
120. L.B. Loeb, *Electrical coronas: their basic physical mechanisms* (Univ of California Press, 2023)
121. P.Y. Tsai, G.W. Qin, L.C. Wadsworth, Theory and techniques of electrostatic charging of melt-blown nonwoven webs. Tappi J. **81**(1), 274–278 (1998)
122. J.A. Giacometti, S. Fedosov, M.M. Costa, Corona charging of polymers: recent advances on constant current charging. Braz. J. Phys. **29**, 269–279 (1999)
123. X. Wang, C. You, Effect of humidity on negative corona discharge of electrostatic precipitators. IEEE Trans. Dielectr. Electr. Insul. **20**(5), 1720–1726 (2013)
124. H. Zhang et al., Design of electret polypropylene melt blown air filtration material containing nucleating agent for effective PM2. 5 capture. RSC advances **8**(15), 7932–7941 (2018)
125. B. Tabti et al., Factors that influence the corona charging of fibrous dielectric materials. J. Electrostat. **67**(2–3), 193–197 (2009)
126. M. Nifuku et al., Charging characteristics for electret filter materials. J. Electrostat. **51**, 200–205 (2001)
127. Q. Sun, W.W.-F. Leung, Charged PVDF multi-layer filters with enhanced filtration performance for filtering nano-aerosols. Sep. Purif. Technol. **212**, 854–876 (2019)
128. R. Thakur, D. Das, A. Das, Optimization study to improve filtration behaviour of electret filter media. J. Textile Institute **107**(11), 1456–1462 (2016)
129. C. Liu et al., Transparent air filter for high-efficiency PM2 5 capture. Nature Commun. **6**(1), 1–9 (2015)
130. Q. Li et al., An electrospun polycarbonate nanofibrous membrane for high efficiency particulate matter filtration. RSC Adv. **6**(69), 65275–65281 (2016)
131. H. Liu et al., High-performance PM0. 3 air filters using self-polarized electret nanofiber/nets. Adv. Funct. Mater. **30**(13), 1909554 (2020)
132. D. Park et al., Light-permeable air filter with self-polarized Nylon-11 nanofibers for enhanced trapping of particulate matters. Adv. Mater. Interfaces **6**(5), 1801832 (2019)
133. S. Lee et al., Reusable polybenzimidazole nanofiber membrane filter for highly breathable PM2. 5 dust proof mask. ACS Appl. Mater. Interfaces **11**(3), 2750–2757 (2019)
134. R. Chen et al., Transparent thermoplastic polyurethane air filters for efficient electrostatic capture of particulate matter pollutants. Nanotechnology **30**(1), 015703 (2018)
135. Y. Li et al., Electrospun nanofibers for high-performance air filtration. Composites Communications **15**, 6–19 (2019)
136. X. Li et al., Electreted polyetherimide–silica fibrous membranes for enhanced filtration of fine particles. J. Colloid Interface Sci. **439**, 12–20 (2015)

137. S. Wang et al., Electret polyvinylidene fluoride nanofibers hybridized by polytetrafluoroethylene nanoparticles for high-efficiency air filtration. ACS Appl. Mater. Interfaces. **8**(36), 23985–23994 (2016)
138. Y. Li et al., All-polymer hybrid electret fibers for high-efficiency and low-resistance filter media. Chem. Eng. J. **398**, 125626 (2020)
139. X. Li et al., Anionic surfactant-triggered Steiner geometrical poly (vinylidene fluoride) nanofiber/nanonet air filter for efficient particulate matter removal. ACS Appl. Mater. Interfaces. **10**(49), 42891–42904 (2018)
140. X. Zhao et al., Low-resistance dual-purpose air filter releasing negative ions and effectively capturing PM2. 5. ACS Appl. Mater. Interfaces **9**(13), 12054–12063 (2017)
141. B.Y. Yeom, E. Shim, B. Pourdeyhimi, Boehmite nanoparticles incorporated electrospun nylon-6 nanofiber web for new electret filter media. Macromol. Res. **18**, 884–890 (2010)
142. H. Gao et al., Electret mechanisms and kinetics of electrospun nanofiber membranes and lifetime in filtration applications in comparison with corona-charged membranes. J. Membr. Sci. **600**, 117879 (2020)
143. Mellouki, H., et al. *Tribo and corona charging and charge decay on polymers plates*. in *2017 5th International Conference on Electrical Engineering-Boumerdes (ICEE-B)*. 2017. IEEE.
144. N. Omran, E. Elnabawy, B. Le, M. Trabelsi, M. Gamal, I. Kandas, A.H. Hassanin, I. Shyha, N. Shehata, Solution blow spun piezoelectric nanofibers membrane for energy harvesting applications. Reactive and Functional Polymers **179**, 105365 (2022)
145. N. Shehata, R. Nair, R. Boualayan, I. Kandas, A. Masrani, E. Elnabawy, N. Omran, M. Gamal, A.H. Hassanin, Stretchable nanofibers of polyvinylidenefluoride (PVDF)/thermoplastic polyurethane (TPU) nanocomposite to support piezoelectric response via mechanical elasticity. Sci. Rep. **12**(1), 8335 (2022)
146. Song, Q., Zhao, R., Liu, T., Gao, L., Su, C., Ye, Y., ... & Huang, W., *One-step vapor deposition of fluorinated polycationic coating to fabricate antifouling and anti-infective textile against drug-resistant bacteria and viruses.* Chemical Engineering Journal,. **418**: 129368 (2021)
147. F.-R. Fan, Z.-Q. Tian, Z.L. Wang, Flexible triboelectric generator. Nano Energy **1**(2), 328–334 (2012)
148. G.Q. Gu et al., Triboelectric nanogenerator enhanced multilayered antibacterial nanofiber air filters for efficient removal of ultrafine particulate matter. Nano Res. **11**(8), 4090–4101 (2018)
149. Y. Feng et al., Self-powered electrostatic filter with enhanced photocatalytic degradation of formaldehyde based on built-in triboelectric nanogenerators. ACS Nano **11**(12), 12411–12418 (2017)
150. G.Q. Gu et al., Triboelectric nanogenerator enhanced nanofiber air filters for efficient particulate matter removal. ACS Nano **11**(6), 6211–6217 (2017)
151. G. Liu et al., Self-powered electrostatic adsorption face mask based on a triboelectric nanogenerator. ACS Appl. Mater. Interfaces. **10**(8), 7126–7133 (2018)
152. B. Ghatak et al., Design of a self-powered triboelectric face mask. Nano Energy **79**, 105387 (2021)
153. C. Luo et al., Preparation and application of high performance PVDF/PS electrospinning film-based triboelectric nanogenerator. Chem. Phys. Lett. **813**, 140276 (2023)
154. Z.L. Wang, J. Song, Piezoelectric nanogenerators based on zinc oxide nanowire arrays. Science **312**(5771), 242–246 (2006)
155. F.R. Fan, W. Tang, Z.L. Wang, Flexible nanogenerators for energy harvesting and self-powered electronics. Adv. Mater. **28**(22), 4283–4305 (2016)
156. M. Mariello et al., Metal-free multilayer hybrid PENG based on soft electrospun/-sprayed membranes with cardanol additive for harvesting energy from surgical face masks. ACS Appl. Mater. Interfaces. **13**(17), 20606–20621 (2021)
157. D.H. Kang, N.K. Kim, H.W. Kang, Electrostatic charge retention in PVDF nanofiber-Nylon mesh multilayer structure for effective fine particulate matter filtration for face masks. Polymers **13**(19), 3235 (2021)
158. A.W. Chin et al., Stability of SARS-CoV-2 in different environmental conditions. The Lancet Microbe **1**(1), e10 (2020)
159. B. Bean et al., Survival of influenza viruses on environmental surfaces. J. Infect. Dis. **146**(1), 47–51 (1982)
160. E. Sánchez-López et al., Metal-based nanoparticles as antimicrobial agents: An overview. Nanomaterials **10**(2), 292 (2020)
161. S.M. Imani et al., Antimicrobial nanomaterials and coatings: Current mechanisms and future perspectives to control the spread of viruses including SARS-CoV-2. ACS Nano **14**(10), 12341–12369 (2020)
162. M.A. Meléndez-Villanueva et al., Virucidal activity of gold nanoparticles synthesized by green chemistry using garlic extract. Viruses **11**(12), 1111 (2019)
163. D. Baram-Pinto et al., Inhibition of HSV-1 attachment, entry, and cell-to-cell spread by functionalized multivalent gold nanoparticles. Small **6**(9), 1044–1050 (2010)
164. S. Gurunathan et al., Antiviral potential of nanoparticles—Can nanoparticles fight against coronaviruses? Nanomaterials **10**(9), 1645 (2020)
165. N. Durán et al., Silver nanoparticles: A new view on mechanistic aspects on antimicrobial activity. Nanomedicine: Nanotechnol Biol Med **12**(3), 789–799 (2016)
166. D. Simões et al., Recent advances on antimicrobial wound dressing: A review. Eur. J. Pharm. Biopharm. **127**, 130–141 (2018)
167. S. Galdiero et al., Silver nanoparticles as potential antiviral agents. Molecules **16**(10), 8894–8918 (2011)
168. Yan, J. and J. Cheng, *Antimicrobial yarn having nanosilver particles and methods for manufacturing the same*. 2005, Google Patents.
169. B. Tang, J. Li, X. Hou, T. Afrin, L. Sun, X. Wang, Colorful and antibacterial silk fiber from anisotropic silver nanoparticles. Industrial & Engineering Chemistry Research **52**(12), 4556–4563 (2013)
170. B. Tang et al., Function improvement of wool fabric based on surface assembly of silica and silver nanoparticles. Chem. Eng. J. **185**, 366–373 (2012)
171. A.P. Richter et al., An environmentally benign antimicrobial nanoparticle based on a silver-infused lignin core. Nat. Nanotechnol. **10**(9), 817–823 (2015)
172. P. Orłowski et al., Antiviral activity of tannic acid modified silver nanoparticles: Potential to activate immune response in herpes genitalis. Viruses **10**(10), 524 (2018)
173. T.Q. Huy et al., Cytotoxicity and antiviral activity of electrochemical–synthesized silver nanoparticles against poliovirus. J. Virol. Methods **241**, 52–57 (2017)
174. M.M. El-Sheekh et al., Antiviral activity of algae biosynthesized silver and gold nanoparticles against herps simplex (HSV-1) virus in vitro using cell-line culture technique. Int. J. Environ. Health Res. **32**(3), 616–627 (2022)
175. C.B. Hiragond et al., Enhanced anti-microbial response of commercial face mask using colloidal silver nanoparticles. Vacuum **156**, 475–482 (2018)
176. G. Borkow et al., A novel anti-influenza copper oxide containing respiratory face mask. PLoS ONE **5**(6), e11295 (2010)
177. L.P. Arendsen, R. Thakar, A.H. Sultan, The use of copper as an antimicrobial agent in health care, including obstetrics and gynecology. Clin. Microbiol. Rev. **32**(4), e00125-e218 (2019)
178. G. Ren et al., Characterisation of copper oxide nanoparticles for antimicrobial applications. Int. J. Antimicrob. Agents **33**(6), 587–590 (2009)

179. P. Ganguly et al., Antimicrobial activity of photocatalysts: Fundamentals, mechanisms, kinetics and recent advances. Appl. Catal. B **225**, 51–75 (2018)
180. S. Akhtar et al., Antibacterial and antiviral potential of colloidal titanium dioxide (TiO2) nanoparticles suitable for biological applications. Materials Research Express **6**(10), 105409 (2019)
181. V. Kumaravel et al., Antimicrobial TiO2 nanocomposite coatings for surfaces, dental and orthopaedic implants. Chem. Eng. J. **416**, 129071 (2021)
182. P. Ekabutr et al., Development of antituberculosis melt-blown polypropylene filters coated with mangosteen extracts for medical face mask applications. Polym. Bull. **76**(4), 1985–2004 (2019)
183. Y.-F. Wang et al., Preparation and characteristic of antibacterial facemasks with Chinese herbal microcapsules. Aerosol and Air Quality Research **17**(8), 2119–2128 (2017)
184. Duong-Quy, S., et al., *The use of exhaled nitric oxide and peak expiratory flow to demonstrate improved breathability and antimicrobial properties of novel face mask made with sustainable filter paper and Folium Plectranthii amboinicii oil: additional option for mask shortage during COVID-19 pandemic.* Multidisciplinary Respiratory Medicine, **15**(1) (2020).
185. K. Chen, X. Qiu, D. Yang, Y. Qian, Amino acid-functionalized polyampholytes as natural broad-spectrum antimicrobial agents for high-efficient personal protection. Green Chem. **22**(19), 6357–6371 (2020)
186. M. Catel-Ferreira et al., Antiviral effects of polyphenols: Development of bio-based cleaning wipes and filters. J. Virol. Methods **212**, 1–7 (2015)
187. B.B. Hsu et al., Mechanism of inactivation of influenza viruses by immobilized hydrophobic polycations. Proc. Natl. Acad. Sci. **108**(1), 61–66 (2011)
188. T. Sinclair et al., Cationically modified membranes using covalent layer-by-layer assembly for antiviral applications in drinking water. J. Membr. Sci. **570**, 494–503 (2019)
189. A.M. Klibanov, Permanently microbicidal materials coatings. J. Mater. Chem. **17**(24), 2479–2482 (2007)
190. F. Gelman, K. Lewis, A.M. Klibanov, Drastically lowering the titer of waterborne bacteriophage PRD1 by exposure to immobilized hydrophobic polycations. Biotech. Lett. **26**, 1695–1700 (2004)
191. A.M. Larson et al., Hydrophobic polycationic coatings disinfect poliovirus and rotavirus solutions. Biotechnol. Bioeng. **108**(3), 720–723 (2011)
192. E. Tuladhar et al., Different virucidal activities of hyperbranched quaternary ammonium coatings on poliovirus and influenza virus. Appl. Environ. Microbiol. **78**(7), 2456–2458 (2012)
193. P.C. DeLeo et al., Assessment of ecological hazards and environmental fate of disinfectant quaternary ammonium compounds. Ecotoxicol. Environ. Saf. **206**, 111116 (2020)
194. M. Martí et al., Protective face mask filter capable of inactivating SARS-CoV-2, and methicillin-resistant Staphylococcus aureus and Staphylococcus epidermidis. Polymers **13**(2), 207 (2021)
195. T. Wang et al., Surface modification of low-density polyethylene films by UV-induced graft copolymerization and its relevance to photolamination. Langmuir **14**(4), 921–927 (1998)
196. J.S. Parent et al., Synthesis and characterization of isobutylene-based ammonium and phosphonium bromide ionomers. Macromolecules **37**(20), 7477–7483 (2004)
197. S. Kumaran et al., Photopolymerizable, universal antimicrobial coating to produce high-performing, multifunctional face masks. Nano Lett. **21**(12), 5422–5429 (2021)
198. Y.L.F. Musico et al., Surface modification of membrane filters using graphene and graphene oxide-based nanomaterials for bacterial inactivation and removal. ACS Sustainable Chemistry & Engineering **2**(7), 1559–1565 (2014)
199. W. Sun, F.G. Wu, Two-dimensional materials for antimicrobial applications Graphene materials and beyond. Chemistry-An Asian Journal **13**(22), 3378–3410 (2018)
200. X. Zou et al., Mechanisms of the antimicrobial activities of graphene materials. J. Am. Chem. Soc. **138**(7), 2064–2077 (2016)
201. B. Ziem et al., Size-dependent inhibition of herpesvirus cellular entry by polyvalent nanoarchitectures. Nanoscale **9**(11), 3774–3783 (2017)
202. H. Zhong et al., Reusable and recyclable graphene masks with outstanding superhydrophobic and photothermal performances. ACS Nano **14**(5), 6213–6221 (2020)
203. J. Zhu et al., Graphene-based antimicrobial polymeric membranes: A review. J. Mater. Chem. A **5**(15), 6776–6793 (2017)
204. H. Zhong et al., Plasmonic and superhydrophobic self-decontaminating N95 respirators. ACS Nano **14**(7), 8846–8854 (2020)
205. S. Bhattacharjee, P. Bahl, A.A. Chughtai, D. Heslop, C.R. MacIntyre, Face masks and respirators: Towards sustainable materials and technologies to overcome the shortcomings and challenges. Nano Select **3**(10), 1355–1381 (2022)
206. A.N. Neely, M.P. Maley, Survival of enterococci and staphylococci on hospital fabrics and plastic. J. Clin. Microbiol. **38**(2), 724–726 (2000)
207. M.C. Sportelli, M. Izzi, E.A. Kukushkina, S.I. Hossain, R.A. Picca, N. Ditaranto, and Cioffi, N, *Can nanotechnology and materials science help the fight against SARS-CoV-2?*. Nanomaterials **10**(4), 802 (2020)
208. S. Djeghdir, A. Peyron, G. Sarry, L. Leclerc, G. Kaouane, P.O. Verhoeven, and Pourchez, J, *Filtration efficiency of medical and community face masks using viral and bacterial bioaerosols*. Sci. Rep. **13**(1), 7115 (2023)
209. H.E. Whyte, A. Joubert, L. Leclerc, G. Sarry, P. Verhoeven, L. Le Coq, and Pourchez, J, *Impact of washing parameters on bacterial filtration efficiency and breathability of community and medical facemasks*. Sci. Rep. **12**(1), 15853 (2022)
210. M.H. Dahanayake, S.S. Athukorala, A.C. Jayasundera, A, *Recent breakthroughs in nanostructured antiviral coating and filtration materials: A brief review*. RSC Adv. **12**(26), 16369–16385 (2022)
211. M. Ebadi, C. McCague, O. Vallee, P.K. Taylor, A.H. Lee, & Bahrami, M, *Salt and surfactant coated filters with antiviral properties and low pressure drop for prospective SARS-CoV2 applications*. Sci. Rep. **12**(1), 11546 (2022)
212. A. Muhammad, A. Kidanemariam, D. Lee, T.T.D. Pham, J. Park,Durability of antimicrobial agent on nanofiber: A collective review from 2018 to 2022. Journal of Industrial and Engineering Chemistry, (2023)
213. I. Rubino, E. Oh, S. Han, S. Kaleem, A. Hornig, S.H. Lee, H.J. Kang, D.H. Lee, K.B. Chu, S. Kumaran, S. Armstrong, Salt coatings functionalize inert membranes into high-performing filters against infectious respiratory diseases. Scientific reports **10**(1), 13875 (2020)
214. S. Han, E. Oh, E. Keltie, J.S. Kim, H.J. Choi, Engineering of materials for respiratory protection: Salt-coated antimicrobial fabrics for their application in respiratory devices. Accounts Mater. Res. **3**(3), 297–308 (2022)
215. E. Oh, S.J. Choi, S. Han, K.H. Lee, H.J. Choi, Highly effective salt-activated alcohol-based disinfectants with enhanced antimicrobial activity. ACS Nano **17**(18), 17811–17825 (2023)
216. E. Horváth, L. Rossi, C. Mercier, C. Lehmann, A. Sienkiewicz, & Forró, L, *Photocatalytic nanowires-based air filter: Towards reusable protective masks*. Adv. Func. Mater. **30**(40), 2004615 (2020)
217. P. Kumar, S. Roy, A. Sarkar, A. Jaiswal, Reusable MoS2-modified antibacterial fabrics with photothermal disinfection properties for repurposing of personal protective masks. ACS Appl. Mater. Interfaces. **13**(11), 12912–12927 (2021)

218. S. Kumaran, E. Oh, S. Han, H. Choi, J, *Photopolymerizable, universal antimicrobial coating to produce high-performing, multifunctional face masks*. Nano Lett. **21**(12), 5422–5429 (2021)
219. Huang, L., Xu, S., Wang, Z., Xue, K., Su, J., Song, Y., ... & Ye, R., *Self-reporting and photothermally enhanced rapid bacterial killing on a laser-induced graphene mask*. ACS nano,. **14**(9): 12045–12053 (2020)
220. X. Zhang, F. Chen, Y. Jiang, Y. Yan, L. Yang, L. Yang, X. Wang, C. Yu, L. Hu, Y. Dai, Q. Wang, Graphene oxide modified microtubular ZnO antibacterial agents for a photocatalytic filter in a facial mask. ACS Applied Nano Materials **5**(11), 16332–16343 (2022)
221. V. Puspasari, A. Ridhova, A. Hermawan, M.I. Amal, M.M. Khan, ZnO-based antimicrobial coatings for biomedical applications. Bioprocess Biosyst. Eng. **45**(9), 1421–1445 (2022)
222. Natsathaporn, P., Herwig, G., Altenried, S., Ren, Q., Rossi, R. M., Crespy, D., & Itel, F., *Functional fiber membranes with antibacterial properties for face masks.* Advanced Fiber Materials, (2023).
223. R. Watson, M. Oldfield, J.A. Bryant, L. Riordan, H.J. Hill, J.A. Watts, M.R. Alexander, M.J. Cox, Z. Stamataki, D.J. Scurr, F. de Cogan, Efficacy of antimicrobial and anti-viral coated air filters to prevent the spread of airborne pathogens. Sci. Rep. **12**, 2803 (2022)
224. R. Wang, Y. Li, Y. Si, F. Wang, Y. Liu, Y. Ma, J. Yu, X. Yin, B. Ding, Rechargeable polyamide-based N-halamine nanofibrous membranes for renewable, high-efficiency, and antibacterial respirators. Nanoscale Adv **1**(5), 1948–1956 (2019)
225. N. El-Atab, R.B. Mishra, M.M. Hussain, Toward nanotechnology-enabled face masks against SARS-CoV-2 and pandemic respiratory diseases. Nanotechnology **33**(6), 062006 (2022)
226. C.G. Kim, S. Lee, M. Kim, V.A. Cao, S.Y. Kim, J. Nah, Synergistic enhancement of filtering efficiency and antibacterial performance of a nanofiber air filter decorated with electropolarized lithium-doped ZnO nanorods. ACS Appl. Mater. Interfaces. **15**(17), 20977–20986 (2023)
227. Vázquez-López, A., Ao, X., del Río Saez, J. S., & Wang, D. Y., *Triboelectric nanogenerator (TENG) enhanced air filtering and face masks: Recent advances.* Nano Energy. 108635 (2023)
228. J.H. Yeh, SP Prakoso, L.L. Santoso, S.J. Chen, B. Chiang, J.C. Cheng, Y.C. Chiu, *A biomass-based electret filter with persistent electrostatic charges for eco-friendly and greener face mask material.* SSRN 4529256
229. S. Zhang, H. Liu, N. Tang, N. Ali, J. Yu, B. Ding, Highly efficient, transparent, and multifunctional air filters using self-assembled 2D nanoarchitectured fibrous networks. Acs. Nano. **13**(11), 13501–13512 (2019)
230. C.L. Li, W.Z. Song, D.J. Sun, M. Zhang, J. Zhang, Y.Q. Chen, S. Ramakrishna, Y.Z. Long, A self-priming air filtration system based on triboelectric nanogenerator for active air purification. Chemical Engineering Journal **452**, 139428 (2023)
231. L.S. Wang, S. Xu, S. Gopal, E. Kim, D. Kim, M. Brier, K. Solanki, J.S. Dordick, Facile fabrication of antibacterial and antiviral perhydrolase-polydopamine composite coatings. Scientific Reports **11**(1), 12410 (2021)
232. Y. Li, Q.M. Pi, H.H. You, J.Q. Li, P.C. Wang, X. Yang, Y. Wu, A smart multi-functional coating based on anti-pathogen micelles tethered with copper nanoparticles via a biosynthesis method using l-vitamin C. RSC Adv. **8**(33), 18272–18283 (2018)
233. F. Tanasa, C.A. Teaca, M. Nechifor, M. Ignat, I.A. Duceac, L. Ignat, Highly specialized textiles with antimicrobial functionality—Advances and challenges. Textiles **3**(2), 219–245 (2023)
234. K. Park, S. Kang, J.W. Park, J. Hwang, Fabrication of silver nanowire coated fibrous air filter medium via a two-step process of electrospinning and electrospray for anti-bioaerosol treatment. Journal of Hazardous Materials **411**, 125043 (2021)
235. Y.N. Chen, Y.H. Hsueh, C.T. Hsieh, D.Y. Tzou, P. Chang, L, *Antiviral activity of graphene–silver nanocomposites against non-enveloped and enveloped viruses*. Int. J. Environ. Res. Public Health **13**(4), 430 (2016)